An Implicitly Extended Crank–Nicolson Scheme for the Heat Equation on a Time-Dependent Domain

Stefan Frei[1] [ORCID] · **Maneesh Kumar Singh[2]**

Abstract

We consider a time-stepping scheme of Crank–Nicolson type for the heat equation on a moving domain in Eulerian coordinates. As the spatial domain varies between subsequent time steps, an extension of the solution from the previous time step is required. Following Lehrenfeld and Olskanskii (ESAIM: M2AN 53(2):585–614, 2019), we apply an implicit extension based on so-called ghost-penalty terms. For spatial discretisation, a cut finite element method is used. We derive a complete a priori error analysis in space and time, which shows in particular second-order convergence in time under a parabolic CFL condition. Finally, we present numerical results in two and three space dimensions that confirm the analytical estimates, even for much larger time steps.

Keywords Eulerian time-stepping scheme · Time-dependent domains · Heat equation · Crank–Nicolson scheme · A priori error analysis

1 Introduction

Partial differential equations (PDEs) posed on moving domains are significant in many areas of science and engineering. They arise for example in flow problems around moving structures, such as pumps [4], wind or water turbines [55], within moving objects [15], or as sub-problems in fluid–structure interactions or multiphase flows. Fluid–structure interactions arise in aerodynamical applications like flow around airplanes or parachutes [59], in biomedical problems such as blood flow through the cardiovascular system [25, 54, 61] or the airflow within the respiratory system [63] and even in tribological applications [47]. Multiphase problems include for instance gas–liquid and particle-laden gas flows [19, 36, 45],

✉ Stefan Frei
stefan.frei@uni-konstanz.de

Maneesh Kumar Singh
maneesh-kumar.singh@imperial.ac.uk

1 Department of Mathematics and Statistics, University of Konstanz, 78457 Konstanz, Germany

2 Department of Mathematics, Imperial College London, London SW7 2AZ, UK

🍊 Springer

rising bubbles [43], droplets in microfluidic devices [17] or the simulation of tumor growth [34]. For further details and applications we refer to the textbooks [3, 35, 56], respectively.

In this article, we consider the time discretisation of a parabolic model problem (namely the heat equation) which is posed on a moving domain $\Omega(t) \subset \mathbb{R}^d$ ($d = 2, 3$) that evolves smoothly in time for $t \in I = [0, t_{max}]$:

$$u_t - \Delta u = f \ \text{ in } \Omega(t), \qquad u = 0 \ \text{ on } \partial\Omega(t), \qquad u(x, 0) = u_0(x) \ \text{ in } \Omega(0). \qquad (1.1)$$

In literature, two major numerical approaches can be found for the simulation of partial differential equations on moving domains: the Arbitrary Lagrangian–Eulerian (ALE) [21, 22] approach, where the equations are transformed to an arbitrary reference domain which is independent of time, and Eulerian approaches, where the equations are solved in the time-dependent Eulerian framework [23, 27, 49].

The ALE approach is a popular technique for the numerical simulation of PDEs on moving domains, in particular for flow problems [41, 42]. For details, we refer to the textbooks [3, 56] and reference cited therein. Convection-diffusion problems on moving domains were, for example, solved in [33, 58] using a stabilised ALE method. The ALE approach is very attractive in the case of moderate domain movements, but shows problems when the shape of the domain changes significantly in time. In particular, topology changes of $\Omega(t)$, as occurring for example in contact problems or considering the separation or union of bubbles can not be modelled by means of an ALE approach [9, 10, 17, 56]. Other examples of extreme variations of $\Omega(t)$ are so-called fingering phenomena, which can be frequently observed in multi-phase flows or even for tumor growth [34].

In such cases, a numerical approach that discretises the equations directly in the moving Eulerian coordinate framework is preferable. The Eulerian framework is also the coordinate framework, which is typically used to model flow problems and consequently, in multi-phase flows [35] and fluid–structure interactions with large displacements [11, 23, 27]. However, as the domains $\Omega(t)$ to be discretised vary with time t, additional difficulties arise concerning a proper and accurate discretisation, both in space and in time.

In recent decades, a great amount of work has been contributed concerning the spatial discretisation of curved or moving boundaries by means of finite elements. The techniques can be categorised in *fitted* and *unfitted* finite element methods. In *fitted* methods, the boundary $\partial\Omega(t)$ is resolved in each time step by the finite element mesh [5, 24, 30]. If the domain is time-dependent, this means that new meshes need to be created in each time step. Several approaches have been proposed to alleviate this issue, such as the locally fitted finite element method [29, 30], which is based on a fixed coarse and a variable fine mesh. However, different issues might arise, such as anisotropic fine cells that complicate the numerical discretisation [28].

The idea in *unfitted* finite element methods, on the other hand, is to use the same finite element mesh for all times t, independently of the position of the boundary $\partial\Omega(t)$. A popular approach is the cut finite element method (CutFEM) [8, 14, 37, 38, 52, 65], where cells of the finite element mesh are cut into parts that lie inside $\Omega(t)$ and parts outside for numerical integration. Dirichlet or Robin boundary conditions are then incorporated weakly by means of Nitsche's method [46, 53]. The method shows similarities to the extended finite element method [16, 20, 32] and the generalised finite element method [2], where the finite element spaces are enriched by suitable functions to account for the position of the boundary.

Much less works can be found in literature concerning a proper time discretisation on moving domains. In the case of moving domains, standard time discretisation based on the method of lines is not directly applicable. The reason is that the domain of definition of the variables changes from time step to time step. As an example consider the finite difference

discretisation of the time derivative within a variational formulation ($\Delta t = t_n - t_{n-1}$)

$$(\partial_t u_h(t_n), \phi_h^n)_{\Omega(t_n)} \approx \frac{1}{\Delta t}(u_h(t_n) - u_h(t_{n-1}), \phi_h^n)_{\Omega(t_n)}.$$

The function $u_h(t_{n-1})$ is only well-defined on $\Omega(t_{n-1})$, but is needed on $\Omega(t_n)$.

A possible remedy is to use characteristic-based approaches based on trajectories that follow the motion of the domain, see e.g. [40]. Similar time-stepping schemes result when applying the ALE method only locally within one time step and projecting back to the original reference frame after each step [18], or based on Galerkin time discretisations with modified Galerkin spaces [31]. The disadvantage of these approaches is the necessity for a projection that needs to be computed within each or after a certain number of steps.

A further alternative are space-time approaches [39, 48], where a $d + 1$-dimensional domain is discretised. These are, however, computationally demanding, in particular within complex three-dimensional applications. The implementation of higher-dimensional discretisations and accurate quadrature formulas pose additional challenges. If a discontinuous Galerkin approach is applied in time for the test functions, the formulation decouples in certain time intervals and can be seen as an Eulerian time-stepping scheme [26, 39, 65].

In this work, we follow a slightly different approach first used by Schott [57] and later analysed by Lehrenfeld & Olshanskii [49]. Here, the idea is to define extensions of the solution $u(t_{n-1})$ from previous time steps to a domain $\Omega_\delta(t_{n-1})$ that spans at least $\Omega(t_n)$. On the finite element level, these extensions can be incorporated implicitly in the time-stepping scheme by so-called *ghost penalty* stabilisations [7] to a sufficiently large domain. These techniques have originally been proposed to extend the coercivity of elliptic bilinear forms from the physical to the computational domain in the context of CutFEM or fictitious domain approaches [7].

Lehrenfeld & Olshanskii [49] analysed the so extended Backward Euler method in detail for a convection-diffusion problem and gave hints on how to transfer the argumentation to the second-order backward difference scheme (BDF2). Recently, the analysis has been extended to higher order in space and time using an isoparametric finite element approach [50]. In [12, 62], extended BDF time-stepping schemes were applied and analysed for the non-stationary Stokes equations on moving domains.

The reason why only BDF-type time-stepping schemes have been considered in previous works, is that in these schemes spatial derivatives appear only on the "new" time step, i.e. $\nabla u(t_n)$. We will see below that the appearance of additional derivatives on $u(t_{n-1})$ will complicate the error analysis severely. This paper gives a first step towards the analysis of time-stepping schemes that require derivatives at different time instants, such as the Crank–Nicolson method, the Fractional-step-θ-, implicit Runge–Kutta- or Adams–Bashforth schemes.

As a first step, we focus in this work on the popular Crank–Nicolson time-stepping scheme. Up to now, it has been largely open, if and under what conditions a Crank–Nicolson-type scheme can be used within an Eulerian time discretisation on moving domains. We give a detailed stability and convergence analysis. While the analysis requires a strong parabolic CFL condition of type $\Delta t \leq ch^{3/2}$, our numerical results indicate that the scheme is stable also for much larger time steps.

The article is organised as follows: In Sect. 2, we introduce the discretisation of the model problem (1.1) in time and space. Section 3 presents a stability analysis for the fully discrete scheme using a CFL condition. In Sect. 4, we show a detailed a priori convergence analysis. Numerical experiments in two and three space dimensions are presented in Sect. 5. Section 6 summarises this article with some concluding remarks.

Fig. 1 Illustration of the domains Ω^n, Ω^{n+1} and the extension Ω_δ^n
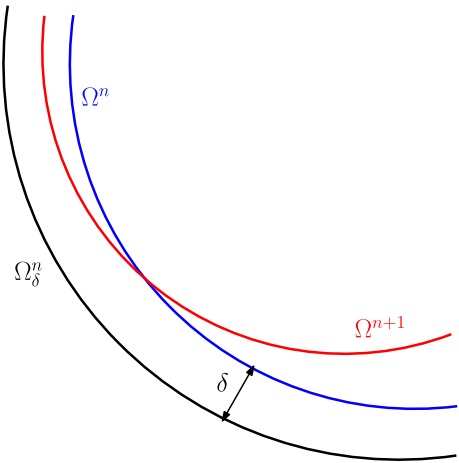
2 Discretisation

In this section, we present the numerical approximation of the model problem (1.1). We start with discretisation in time and continue with the spatial discretisation of the resulting time-discrete formulation.

2.1 Temporal Discretisation

For time discretisation, we divide the time interval of interest $I = [0, t_{max}]$ in intervals $I_n = (t_{n-1}, t_n]$. For simplicity, we take a uniform time step $\Delta t = \dfrac{t_{max}}{N}$ and define $t_n = n\Delta t$. We define the domain $\Omega^n := \Omega(t_n)$ with boundary $\Gamma^n := \Gamma(t_n)$ and write $u^n = u(t_n)$ for the exact solution of the continuous problem (1.1) at time t_n.

A δ-neighborhood of $\Omega(t)$ at time step n is chosen large enough such that $(\Omega^n \cup \Omega^{n+1}) \subset \Omega_\delta^n$, see Fig. 1. Therefore we choose

$$\delta \geq w_{max}\Delta t, \qquad w_{max} = \sup_{t \in I,\, x \in \partial\Omega(0)} \|\partial_t T(x, t) \cdot n\|.$$

The required regularity of the domain mapping T will be ensured in Assumption 1 below. For the error analysis, we will also assume the upper bound

$$\delta \leq c_\delta w_{max}\Delta t \tag{2.1}$$

with a constant $c_\delta > 1$. Finally, we introduce the following notations for some space-time domains

$$Q := \bigcup_{t \in I} \{t\} \times \Omega(t), \quad Q^n := \bigcup_{t \in I_n} \{t\} \times \Omega(t)$$

$$Q_\delta^n := \bigcup_{t \in I_n} \{t\} \times \Omega_\delta(t), \quad \hat{Q} = \Omega(0) \times [0, t_{max}].$$

Now, the Crank–Nicolson method applied to (1.1) writes formally

$$\frac{u^n - u^{n-1}}{\Delta t} - \frac{1}{2}(\Delta u^n + \Delta u^{n-1}) = \frac{1}{2}(f^n + f^{n-1}), \quad x \in \Omega^n. \tag{2.2}$$

The main issue of this formulation is that u^{n-1} is needed on Ω^n, while it is defined on Ω^{n-1}. Thus, we will add implicit extension operators below to define u^n on $\Omega^n_\delta \supset \Omega^{n+1}$, where it is needed in the following time step. Similarly, f^{n-1} might be undefined on $\Omega^n \setminus \Omega^{n-1}$. If f^{n-1} is given analytically, it can typically be extended in a canonical way to Ω^n. To cover different scenarios, we do not want to restrict the analysis in this work to a particular extension, but assume only that f^{n-1} is smoothly extended to Ω^n.

In this article, we will use the abbreviation c to refer to a generic positive constant, which is independent of discretisation parameters (Δt, h) and the relative positions of the boundary with respect to the mesh.

2.1.1 Extension Operator

In this part, we introduce an extension operator to extend variables, for example the exact solution u, to larger domains as the spatial domain evolves. We make the following assumption (see also [12, Assumption 3.2]) for the analysis of this article.

Assumption 1 The boundary of the initial domain $\Omega(0)$ is assumed to be piecewise smooth and Lipschitz, and the domain motion $T(t)$ is a $W^{1,\infty}$-diffeomorphism for each t, that fulfills $T \in W^{r,\infty}(\hat{Q})$, where $r = \max\{3, m+1\}$ and m is the polynomial degree of the finite element space defined in the following subsection.

By using Assumption 1, there exist $W^{r,\infty}$-stable extension operators E^n from Ω^n to Ω^n_δ that satisfy the following analytical properties:

$$\|E^n u - u\|_{W^{m+1,p}(\Omega^n)} = 0, \quad \|E^n u\|_{W^{m+1,p}(\Omega^n_\delta)} \le c\|u\|_{W^{m+1,p}(\Omega^n)}, \qquad (2.3)$$

$$\|\partial_t E^n u\|_{H^m(\Omega^n_\delta)} \le c\left(\|u\|_{H^{m+1}(\Omega^n)} + \|\partial_t u\|_{H^m(\Omega^n)}\right), \qquad (2.4)$$

$$\|\partial_t^3 E^n u\|_{L^\infty(Q^n_\delta)} \le c\|u\|_{W^{3,\infty}(Q)}. \qquad (2.5)$$

The properties (2.3) and (2.4) are discussed in [12]. In an analogous way, one can derive the estimate for the third-order time derivative in (2.5). These extension operators will be used throughout the article, whenever functions would be undefined on parts of the domain where they are needed.

2.2 Spatial Discretisation

For spatial discretisation, we introduce a polygonal domain D, which is chosen large enough, such that $\Omega^n_\delta \subset D$ for all n. We introduce a quasi-uniform (i.e., shape- and size-regular) family of triangulations $(\mathcal{T}_h)_{h>0}$ of D with maximum cell size h (see, e.g., [6, Section 4.4]), which will serve as background meshes.

In each time step, we extract from $\mathcal{T}_h$ all cells of non-empty intersection with Ω^n_δ and define

$$\mathcal{T}^n_{h,\delta} := \{K \in \mathcal{T}_h : K \cap \Omega^n_\delta \ne \emptyset\}.$$

We write $\Omega^n_{h,\delta}$ for the domain spanned by all cells $K \in \mathcal{T}^n_{h,\delta}$ and define the following finite element space:

$$V^{n,m}_h := \{v \in C(\Omega^n_{h,\delta}), v|_K \in P_m(K) \ \forall K \in \mathcal{T}^n_{h,\delta}\}, \quad m \ge 1.$$
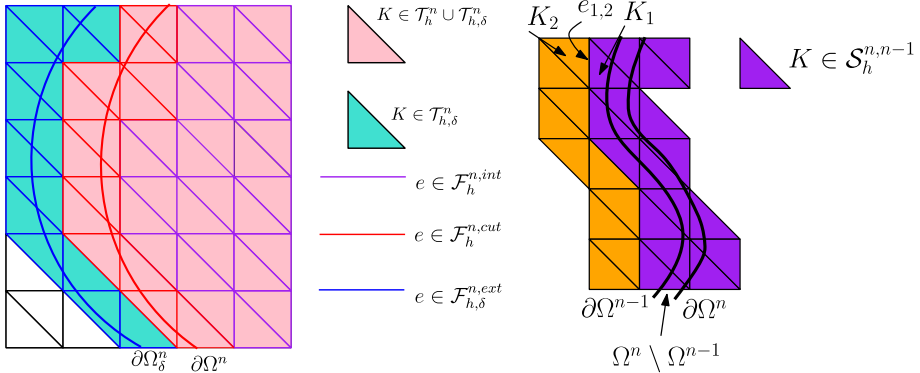
Fig. 2 Left: Illustration of the triangulations $\mathcal{T}_h^n$ and $\mathcal{T}_{h,\delta}^n$ and the sets of facets $\mathcal{F}_{h,\delta}^n = \mathcal{F}_{h,\delta}^{n,int} \cup \mathcal{F}_{h,\delta}^{n,cut} \cup \mathcal{F}_{h,\delta}^{n,ext}$. Right: Set of boundary cells $\mathcal{S}_h^{n,n-1}$

The set of elements that lie (at least partially) outside of Ω^{n-1}, but in Ω^n, will be of particular interest in the analysis. The domain spanned by them will be denoted by

$$\mathcal{S}_h^{n,n-1} := \bigcup_{K \in \mathcal{T}_h^{n,n-1}} K, \quad \text{where } \mathcal{T}_h^{n,n-1} := \left\{ K \in \mathcal{T}_{h,\delta}^n, \ K \cap (\Omega^n \setminus \Omega^{n-1}) \neq \emptyset \right\}.$$

Moreover, we introduce the following notations for the facets of $\mathcal{T}_{h,\delta}^n$, see Fig. 2 for an illustration:

- $\mathcal{F}_{h,\delta}^n$: the set of interior facets of $\mathcal{T}_{h,\delta}^n$.
- $\mathcal{F}_{h,\delta}^{n,int}$: the set of facets that belong exclusively to elements $K \in \mathcal{T}_{h,\delta}^n$ that lie completely in the interior of Ω^n.
- $\mathcal{F}_{h,\delta}^{n,cut}$: the set of facets that belong to some element $K \in \mathcal{T}_{h,\delta}^n$ with $K \cap \partial\Omega^n \neq \emptyset$.
- $\mathcal{F}_{h,\delta}^{n,ext}$: the set of remaining facets of $\mathcal{F}_{h,\delta}^n$, i.e. $\mathcal{F}_{h,\delta}^{n,ext} := \mathcal{F}_{h,\delta}^n \setminus \left(\mathcal{F}_{h,\delta}^{n,int} \cup \mathcal{F}_{h,\delta}^{n,cut} \right)$
- $\mathcal{F}_{h,\delta}^{n,g} := \mathcal{F}_{h,\delta}^{n,cut} \cup \mathcal{F}_{h,\delta}^{n,ext}$.

Assumption 2 *(CFL condition)* We assume the CFL condition $\Delta t \leq c_{CFL} h^{3/2}$ for a sufficiently small constant c_{CFL}.

The inequality (2.1) and the CFL condition (Assumption 2) lead to

$$\delta \leq c_\delta w_{max} \Delta t \leq c w_{max} h^{3/2}. \tag{2.6}$$

Remark 2.1 The inequality (2.6) implies that the distance between $\partial\Omega^n$ and $\partial\Omega^{n-1}$ is bounded by $\mathcal{O}(h^{3/2})$. This implies the following property, which will be needed in the analysis below: For each cell $K \in \mathcal{S}_h^{n,n-1}$, there exists a path of cells K_i, $i = 1, \ldots, M$, such that $\overline{K_i} \cap \overline{K_{i+1}}$ is a facet in $\mathcal{F}_{h,\delta}^{n,g} \cap \mathcal{F}_{h,\delta}^{n-1,g}$ and the final cell K_M lies fully in the interior of Ω^n. Furthermore, the number of cases, in which an element $K_M \subset \Omega^n$ is utilised as a final element among all paths, can be bounded independently of h and Δt.

2.2.1 Discrete Variational Formulation

In the numerical approximation, the boundary condition of the discrete problem (2.7) is implemented weakly by means of Nitsche's method. Moreover, the function u_h^n is extended

by means of a ghost penalty term $g_h^n(\cdot, \cdot)$. In each time step $n = 1, 2, \ldots, N$, we consider the following discrete variational formulation: Find $u_h^n \in V_h^{n,m}$ such that

$$\mathcal{A}(u_h^n, u_h^{n-1}; v_h) = (f_h^{n-\frac{1}{2}}, v_h), \quad \forall v_h \in V_h^{n,m}, \tag{2.7}$$

where

$$\mathcal{A}(u_h^n, u_h^{n-1}; v_h) := \left(D_{\Delta t}^- u_h^n, v_h\right)_{\Omega^n} + \frac{1}{2} a_h^n(u_h^n, v_h) + \frac{1}{2} a_h^n(u_h^{n-1}, v_h) + \frac{\gamma_D}{h}(u_h^n, v_h)_{\partial\Omega^n}$$
$$+ \gamma_g g_h^n(u_h^n, v_h) \tag{2.8}$$

and

$$D_{\Delta t}^- u_h^n = \frac{u_h^n - u_h^{n-1}}{\Delta t}, \quad a_h^n(u_h^k, v_h) = (\nabla u_h^k, \nabla v_h)_{\Omega^n} - (\partial_n u_h^k, v_h)_{\partial\Omega^n},$$
$$f^{n-\frac{1}{2}} = \frac{f^n + f^{n-1}}{2}.$$

We assume that all integrals in (2.8) are evaluated exactly. For a consideration of additional quadrature errors, that result when cut cells are approximated linearly in the computation of the integrals, we refer to [49].

We would like to stress that the Nitsche penalty term $\frac{\gamma_D}{h}(u_h^n, v_h)_{\partial\Omega^n}$ is evaluated only at the new time step (superscript n). Moreover, we consider here a non-symmetric version of Nitsche's method, i.e., without the symmetry term $-(u_h^k, \partial_n v_h)_{\partial\Omega^n}$ in $a_h^n(u_h^k, v_h)$. This form of the Nitsche penalty term will be necessary for the following stability analysis, see Remark 3.7. The symmetry term is left out, as it would lead to a significantly larger consistency error, which would dominate the overall error, see Remark 4.3.

The ghost penalty stabilization is defined by

$$g_h^n(w_h, v_h) = \sum_{e \in \mathcal{F}_{h,\delta}^{n,g}} \sum_{k=1}^m \frac{h^{2k-1}}{k!^2} \int_e [[\partial_n^k w_h]] \cdot [[\partial_n^k v_h]] \, ds, \tag{2.9}$$

where $[[\cdot]]$ is the jump operator and ∂_n the exterior normal derivative. For further possibilities for the extension g_h^n, we refer to [49]. The variant chosen here based on the jump of derivatives over edges has the advantage that it is fully consistent, in the sense that $g_h^n(u, v)$ vanishes for $u \in H^{m+1}(\Omega_\delta^n)$. The purpose of the ghost penalty is twofold: First, it serves to extend the solution u_h^n implicitly to $\Omega_{h,\delta}^n$. Secondly, it ensures the discrete coercivity of the formulation (2.7) on $\mathcal{T}_{h,\delta}^n$.

To incorporate the initial condition, we set $u_h^0 := E^1 u^0$ in (2.8) for $n = 1$, where $E^1 u^0$ is a smooth, e.g. a canonical extension, of the initial value u_0. This corresponds to the following Ritz projection of the initial value u^0

$$\Delta t^{-1}(u_h^0, v_h)_{\Omega^1} + a^1(u_h^0, v_h) = \Delta t^{-1}(E^1 u^0, v_h)_{\Omega^1} + a^1(E^1 u^0, v_h) \quad \forall v_h \in V_h^1,$$

The following lemma is the key to extend the discrete coercivity to Ω_δ^n:

Lemma 2.2 *Given Assumption 2, any discrete function $v_h^n \in V_h^{n,m}$ satisfies*

$$\|v_h^n\|_{\Omega_{h,\delta}^n}^2 \le c\|v_h^n\|_{\Omega^n}^2 + ch^2 g_h^n(v_h, v_h), \qquad \|\nabla v_h^n\|_{\Omega_{h,\delta}^n}^2 \le c\|\nabla v_h^n\|_{\Omega^n}^2 + cg_h^n(v_h, v_h).$$

In addition, for $v \in H^{m+1}(\Omega_\delta^n)$, $m \ge 1$, it holds

$$g_h^n(v, v) \le ch^{2m}\|v\|_{H^{m+1}(\Omega_\delta^n)}^2.$$

Proof A proof of this lemma is given in [49]. □

At the end of this section, we briefly show that the variational formulation (2.7) is well-posed for each n. We define the discrete energy as

$$\mathfrak{E}^n(u_h^n, u_h^{n-1}) = \left(\frac{1}{2}\|\nabla u_h^n + \nabla u_h^{n-1}\|_{\Omega^n}^2 + \frac{1}{\Delta t}\|u_h^n - u_h^{n-1}\|_{\Omega^n}^2 + \frac{\gamma_D}{h}\|u_h^n\|_{\partial\Omega^n}^2 + \gamma_g g_h^n(u_h^n, u_h^n) \right)^{1/2}.$$
(2.10)

and the energy norm as

$$|||u_h^n|||_n := \mathfrak{E}^n(u_h^n, 0).$$

We will show the coercivity relation

$$|||u_h^n|||_n^2 \leq \frac{1}{4}\mathcal{A}(u_h^n, 0; u_h^n), \qquad u_h^n \in V_h^{m,n}.$$
(2.11)

for sufficiently large γ_g, γ_D. The well-posedness of (2.7) follows then by standard arguments.

From the definition of the bilinear form $\mathcal{A}(u_h^n, 0; u_h^n)$, we have

$$\mathcal{A}(u_h^n, 0; u_h^n) = \frac{1}{\Delta t}\|u_h^n\|_{\Omega^n}^2 + \frac{1}{2}\|\nabla u_h^n\|_{\Omega^n}^2 - \frac{1}{2}(\partial_n u_h^n, u_h^n)_{\partial\Omega^n} + \frac{\gamma_D}{h}\|u_h^n\|_{\partial\Omega^n}^2 + \gamma_g g_h^n(u_h^n, u_h^n).$$

The term $-\frac{1}{2}(\partial_n u_h^n, u_h^n)_{\partial\Omega^n}$ is estimated by means of Young's inequality and an inverse inequality as follows for sufficiently small $\epsilon > 0$:

$$-\frac{1}{2}(\partial_n u_h^n, u_h^n)_{\partial\Omega^n} \geq -\frac{\epsilon h}{4}\|\nabla u_h^n\|_{\partial\Omega^n}^2 - \frac{1}{4\epsilon h}\|u_h^n\|_{\partial\Omega^n}^2$$

$$\geq -c\epsilon\|\nabla u_h^n\|_{\Omega_h^n}^2 - \frac{1}{4\epsilon h}\|u_h^n\|_{\partial\Omega^n}^2.$$

For sufficiently large parameters γ_D, γ_g, we have using Lemma 2.2

$$-\frac{1}{2}(\partial_n u_h^n, u_h^n)_{\partial\Omega^n} \geq -\frac{1}{4}\left(\|\nabla u_h^n\|_{\Omega^n}^2 + \gamma_g g_h^n(u_h^n, u_h^n) \right) - \frac{\gamma_D}{4h}\|u_h^n\|_{\partial\Omega^n}^2.$$

This proves the coercivity (2.11).

Remark 2.3 The analysis given in this article can be generalised to the non-stationary convection-diffusion problem

$$\partial_t u + b \cdot \nabla u - \Delta u = f \qquad \text{in } \Omega$$

for a bounded function $b \in L^\infty(Q)$. The corresponding bilinear form includes the additional term $\frac{1}{2}(b \cdot \nabla(u^n + u^{n-1}), v)_{\Omega^n}$. In the coercivity proof, as well as the stability analysis given below, this term can be estimated by estimates of type

$$(b \cdot \nabla(u^n + u^{n-1}), u^n)_{\Omega^n} \leq \|b\|_{L^\infty(Q)}\|\nabla(u^n + u^{n-1})\|_{\Omega^n}\|u^n\|_{\Omega^n}$$

$$\leq \epsilon\|\nabla(u^n + u^{n-1})\|_{\Omega^n}^2 + c_b\epsilon^{-1}\|u^n\|_{\Omega^n}^2$$

for $c_b := \|b\|_{L^\infty(Q)}$ and $\epsilon > 0$. Control over the latter term can be obtained by means of the discrete time derivative (namely $\frac{1}{\Delta t}(u^n - u^{n-1}, u^n)$). However, in order to keep the analysis as simple and concise as possible, we will in the following not consider this additional convective term.

3 Stability Analysis

In this section, a detailed stability analysis of the discrete problem (2.7) is developed. One of the main issues in the analysis is that the discrete functions u_h^{n-1} and ∇u_h^{n-1} appear on Ω^n in the n-th time step, whereas bounds are only available for $\|u_h^{n-1}\|_{\Omega^{n-1}}$ and $\|\nabla u_h^{n-1}\|_{\Omega^{n-1}}$ from the previous time step. We start with some technical lemmas that will enable us to deal with this issue.

3.1 Auxiliary Estimates

We start with a lemma that uses the smallness of the mismatch $\Omega^n \setminus \Omega^{n-1}$ compared to the set of cells $\mathcal{S}_h^{n,n-1}$ that contains this area, see Fig. 2.

Lemma 3.1 *Any discrete functions $v_h^n \in V_h^{n,m}$, $v_h^{n-1} \in V_h^{n-1,m}$ satisfy the following inequality:*

$$\|\nabla v_h^n - \nabla v_h^{n-1}\|_{\Omega^n \setminus \Omega^{n-1}}^2 \leq c \frac{\Delta t}{h} \|\nabla v_h^n - \nabla v_h^{n-1}\|_{\mathcal{S}_h^{n,n-1}}^2. \tag{3.1}$$

Proof Let $T \in \mathcal{T}_h^{n,n-1}$ and $S_T := T \cap (\Omega^n \setminus \Omega^{n-1})$. Due to the quasi-uniformity of the background mesh, we have $|T| \geq ch^d$ and from (2.1) $|S_T| = |T \cap (\Omega^n \setminus \Omega^{n-1})| \leq ch^{d-1}\Delta t$. We show the estimate on the reference element (the unit simplex $\hat{T}$) using the linear bijective map $\xi_T : \hat{T} \to T$. Let $p := (\nabla v_h^n - \nabla v_h^{n-1})|_T$, $\hat{p} = p \circ \xi_T$ and $\hat{S}_T := \xi_T^{-1}(S_T)$. As the map ξ_T is linear, we have by integral transformation

$$|\hat{S}_T| = \int_{\hat{S}_T} 1 \, d\hat{x} = \int_{S_T} |\det(\nabla \xi_T^{-1})| \, dx = |S_T| \frac{|\hat{T}|}{|T|} \leq c \frac{\Delta t}{h}. \tag{3.2}$$

Similarly, it holds that

$$\|p\|_{S_T} \leq c|T|^{1/2}\|\hat{p}\|_{\hat{S}_T} \quad \text{and} \quad \|\hat{p}\|_{\hat{T}} \leq c|T|^{-1/2}\|p\|_T. \tag{3.3}$$

On the reference simplex, we use equivalence of norms for the polynomial $\hat{p}$

$$\|\hat{p}\|_{\hat{S}_T} \leq |\hat{S}_T|^{1/2}\|\hat{p}\|_{\infty,\hat{T}} \leq c|\hat{S}_T|^{1/2}\|\hat{p}\|_{\hat{T}}. \tag{3.4}$$

Combination of (3.3) and (3.4) yields $\|p\|_{S_T} \leq c|\hat{S}_T|^{1/2}\|p\|_T$. After using (3.2), summation over all cells $T \in \mathcal{T}_h^{n,n-1}$ completes the proof.

Lemma 3.2 *Let Assumptions 2 be valid. Any discrete functions $v_h^n \in V_h^{n,m}$, $v_h^{n-1} \in V_h^{n-1,m}$ satisfy the following inequality:*

$$\|\nabla v_h^n - \nabla v_h^{n-1}\|_{\Omega^n \setminus \Omega^{n-1}}^2 \leq \frac{2}{\Delta t} \|v_h^n - v_h^{n-1}\|_{\Omega^n}^2 + cg_h^n(v_h^n, v_h^n) + cg_h^{n-1}(v_h^{n-1}, v_h^{n-1}). \tag{3.5}$$

Proof By Lemma 3.1 we have that

$$\|\nabla v_h^n - \nabla v_h^{n-1}\|_{\Omega^n \setminus \Omega^{n-1}}^2 \leq c \frac{\Delta t}{h} \|\nabla v_h^n - \nabla v_h^{n-1}\|_{\mathcal{S}_h^{n,n-1}}^2. \tag{3.6}$$

Now let $K_1 \in \mathcal{S}_h^{n,n-1}$. By Remark 2.1, there is a set of neighbouring cells $K_2, ..., K_M$, such that $(\overline{K}_i \cap \overline{K}_{i+1}) \in (\mathcal{F}_{h,\delta}^{n,g} \cap \mathcal{F}_{h,\delta}^{n-1,g})$ and K_M lies fully in the interior of Ω^n. Let $e_{1,2}$ be the

edge that separates the cells K_1 and K_2, see Fig. 2. Then, using arguments from [51, Lemma 5.1] and [49, Lemma 5.2], we can deduce that

$$\|\nabla v_h^n - \nabla v_h^{n-1}\|_{K_1}^2 \le c_0 \|\nabla v_h^n - \nabla v_h^{n-1}\|_{K_2}^2 + c \sum_{k=1}^m \int_{e_{1,2}} h^{2k-1} [[\partial_n^k v_h^n - \partial_n^k v_h^{n-1}]]^2 ds$$

$$\le c_0 \|\nabla v_h^n - \nabla v_h^{n-1}\|_{K_2}^2 + c \sum_{k=1}^m \int_{e_{1,2}} h^{2k-1} [[\partial_n^k v_h^n]]^2 ds + c \int_{e_{1,2}} h^{2k-1} [[\partial_n^k v_h^{n-1}]]^2 ds,$$

(3.7)

with a constant c_0 that depends solely on the polynomial degree m and the shape-regularity of the triangulations [51, Lemma 5.1]. We follow this process from K_2 to K_M by crossing edges $e_{2,3}$ to $e_{M-1,M}$ to obtain

$$\|\nabla v_h^n - \nabla v_h^{n-1}\|_{K_1}^2 \le c_0^M \|\nabla v_h^n - \nabla v_h^{n-1}\|_{K_M}^2$$
$$+ c \sum_{k=1}^m \sum_{j=2}^M \left(\int_{e_{j-1,j}} h^{2k-1} [[\partial_n^k v_h^n]]^2 ds + \int_{e_{j-1,j}} h^{2k-1} [[\partial_n^k v_h^{n-1}]]^2 ds \right).$$

(3.8)

For the first term on the right-hand side of (3.8), we use an inverse inequality with constant c_{inv}

$$c_0^M \frac{\Delta t}{h} \|\nabla v_h^n - \nabla v_h^{n-1}\|_{K_M}^2 \le \frac{c_0^M c_{\text{inv}}^2 \Delta t}{h^3} \|v_h^n - v_h^{n-1}\|_{K_M}^2 \qquad (3.9)$$

As all edges $e_{j-1,j}$ belong to both $\mathcal{F}_{h,\delta}^{n,g}$ and $\mathcal{F}_{h,\delta}^{n-1,g}$, we obtain after summation over all cells in $\mathcal{S}_h^{n,n-1}$ from (3.6), (3.8) and (3.9)

$$\|\nabla v_h^n - \nabla v_h^{n-1}\|_{\Omega^n \setminus \Omega^{n-1}}^2 \le c_0^M c_{\text{inv}}^2 \frac{\Delta t}{h^3} \|v_h^n - v_h^{n-1}\|_{\Omega^n}^2$$
$$+ c \frac{\Delta t}{h} \left(g_h^n(v_h^n, v_h^n) + g_h^{n-1}(v_h^{n-1}, v_h^{n-1}) \right).$$

Using the CFL condition $\Delta t \le c_{\text{CFL}} h^{3/2}$ for sufficiently small $c_{\text{CFL}} \le \sqrt{2/c_0^M c_{\text{inv}}^2}$, we obtain $c_0^M c_{\text{inv}}^2 \frac{\Delta t}{h^3} \le \frac{2}{\Delta t}$ and $\Delta t/h \le c$, which completes the proof. □

We note that the CFL condition is required to estimate the "mismatch" $\|\nabla v_h^{n-1}\|_{\Omega^n \setminus \Omega^{n-1}}^2$ by means of the discrete time derivative $\frac{1}{\Delta t}\|v_h^n - v_h^{n-1}\|_{\Omega^n}^2$ (see the following lemma). The constant c_{CFL} depends on constants c_0 and c_{inv} that depend on polynomial degree m and shape-regularity of the triangulations.

Next, we discuss how the term $\|\nabla u_h^{n-1}\|_{\Omega^n}$ can be bounded by $\|\nabla u_h^{n-1}\|_{\Omega^{n-1}}$ along with additional terms that can be controlled in the following stability analysis.

Lemma 3.3 *Under the assumptions of Lemma 3.2 it holds for $v_h^n \in V_h^{n,m}$, $v_h^{n-1} \in V_h^{n-1,m}$ and $l \in \{n-1, n\}$ that*

$$\Delta t \|\nabla v_h^l\|_{\Omega^n \setminus \Omega^{n-1}}^2 \le \frac{\Delta t}{2} \|\nabla v_h^n + \nabla v_h^{n-1}\|_{\Omega^n \setminus \Omega^{n-1}}^2 + \|v_h^n - v_h^{n-1}\|_{\Omega^n}^2$$
$$+ c \Delta t g_h^n(v_h^n, v_h^n) + c \Delta t g_h^{n-1}(v_h^{n-1}, v_h^{n-1}).$$

(3.10)

Proof By the triangle inequality, we have

$$\|\nabla v_h^{n-1}\|_{\Omega^n \setminus \Omega^{n-1}} \le \frac{1}{2} \|\nabla v_h^n + \nabla v_h^{n-1}\|_{\Omega^n \setminus \Omega^{n-1}} + \frac{1}{2} \|\nabla v_h^n - \nabla v_h^{n-1}\|_{\Omega^n \setminus \Omega^{n-1}}.$$

By means of the inequality $(a+b)^2 \leq 2a^2 + 2b^2$ this implies

$$\Delta t \|\nabla v_h^{n-1}\|_{\Omega^n \setminus \Omega^{n-1}}^2 \leq \frac{\Delta t}{2} \|\nabla v_h^n + \nabla v_h^{n-1}\|_{\Omega^n \setminus \Omega^{n-1}}^2 + \frac{\Delta t}{2} \|\nabla v_h^n - \nabla v_h^{n-1}\|_{\Omega^n \setminus \Omega^{n-1}}^2. \quad (3.11)$$

The statement follows by using Lemma 3.2 for the second term in (3.11)

$$\frac{\Delta t}{2} \|\nabla v_h^n - \nabla v_h^{n-1}\|_{\Omega^n \setminus \Omega^{n-1}}^2 \leq \|v_h^n - v_h^{n-1}\|_{\Omega^n}^2 + c\Delta t g_h^n(v_h^n, v_h^n) + c\Delta t g_h^{n-1}(v_h^{n-1}, v_h^{n-1}). \quad (3.12)$$

□

Next, we provide the following Poincaré-type estimate:

Lemma 3.4 *Let $u \in W^{1,p}(\Omega)$ for $1 \leq p < \infty$ and let the CFL condition (Assumption 2) be valid. It holds for $l \in \{n-1, n\}$*

$$\|u\|_{L^p(\Omega^n \setminus \Omega^{n-1})}^p \leq c\Delta t \|u\|_{L^p(\partial \Omega^l)}^p + c\Delta t^2 \|\nabla u\|_{L^p(\Omega^n \setminus \Omega^{n-1})}^p. \quad (3.13)$$

Proof The proof follows the lines of [56, Lemma 4.34] and uses the fact that dist$(\Omega^n, \Omega^{n-1}) \leq c\Delta t$. □

Using this, we can derive bounds for $\|v_h^{n-1}\|_{\Omega^n \setminus \Omega^{n-1}}^2$ and $\|v_h^n\|_{\Omega^n \setminus \Omega^{n-1}}^2$:

Lemma 3.5 *Under the assumptions of Lemma 3.2 it holds for $v_h^l \in V_h^{l,m}$, $l \in \{n-1, n\}$*

$$\|v_h^l\|_{\Omega^n \setminus \Omega^{n-1}}^2 \leq c\Big(\Delta t \|v_h^l\|_{\partial \Omega^l}^2 + \Delta t \|v_h^n - v_h^{n-1}\|_{\Omega^n}^2 + \Delta t^2 \|\nabla v_h^n + \nabla v_h^{n-1}\|_{\Omega^n}^2$$
$$+ \Delta t^2 g_h^{n-1}(v_h^{n-1}, v_h^{n-1}) + \Delta t^2 g_h^n(v_h^n, v_h^n)\Big) \quad (3.14)$$

Proof By means of Lemma 3.4 for $p = 2$ we have for $l \in \{n-1, n\}$

$$\|v_h^l\|_{\Omega^n \setminus \Omega^{n-1}}^2 \leq c\Delta t \|v_h^l\|_{\partial \Omega^l}^2 + c\Delta t^2 \|\nabla v_h^l\|_{\Omega^n \setminus \Omega^{n-1}}^2 \quad (3.15)$$

The statement follows by applying Lemma 3.3 to the second term in (3.15). □

3.2 Stability Result

Before discussing the stability result, we introduce some abbreviations for the space-time Bochner norms to simplify the mathematical expressions

$$\|u\|_{\infty,m,I_k} := \|u\|_{L^\infty(I_k, H^m(\Omega(t)))}, \qquad \|u\|_{\infty,m} := \|u\|_{\infty,m,I}, \quad (3.16)$$

where $m \in \mathbb{N} \cup \{0\}$ and $H^0(\Omega(t)) := L^2(\Omega(t))$. We prove the following stability result.

Theorem 3.6 (Stability) *Let Assumptions 2 be valid and let $f \in L^\infty(I, L^2(\Omega(t)))$, $u^0 \in H^1(\Omega^0)$ and let the mapping T be a $W^{1,\infty}$-diffeomorphism. For sufficiently large γ_g and γ_D the solution $\{u_h^k\}_{k=1}^n$ of the discrete problem (2.7) fulfills*

$$\|u_h^n\|_{\Omega^n}^2 + \Delta t \|u_h^n\|_{\Omega^n}^2 + \Delta t \sum_{k=1}^n \mathfrak{E}^k(u_h^k, u_h^{k-1})$$
$$\leq c \exp(c\, t_n) \left(\|u^0\|_{\Omega^0}^2 + \Delta t \|\nabla u^0\|_{\Omega^0}^2 + t_n \|f\|_{\infty,0}^2 \right), \quad (3.17)$$

with $\mathfrak{E}^k(\cdot, \cdot)$ defined in (2.10).

Proof We test (2.7) with $v_h = 2\Delta t u_h^n$ to obtain

$$2\left(u_h^n - u_h^{n-1}, u_h^n\right)_{\Omega^n} + \Delta t\left(\nabla u_h^n + \nabla u_h^{n-1}, \nabla u_h^n\right)_{\Omega^n} + \frac{2\gamma_D \Delta t}{h}(u_h^n, u_h^n)_{\partial\Omega^n}$$
$$-\Delta t(\partial_n u_h^n + \partial_n u_h^{n-1}, u_h^n)_{\partial\Omega^n} + 2\Delta t\gamma_g g_h^n(u_h^n, u_h^n) = 2\Delta t(f^{n-\frac{1}{2}}, u_h^n). \tag{3.18}$$

We estimate the fourth term in (3.18) by means of Young's inequality with a sufficiently small $\epsilon > 0$ followed by an inverse inequality

$$\Delta t(\partial_n u_h^n + \partial_n u_h^{n-1}, u_h^n)_{\partial\Omega^n} \le \frac{\Delta t \epsilon h}{16}\|\partial_n u_h^n + \partial_n u_h^{n-1}\|_{\partial\Omega^n}^2 + \frac{4\Delta t}{\epsilon h}\|u_h^n\|_{\partial\Omega^n}^2$$
$$\le \frac{\Delta t}{16}\|\nabla u_h^n + \nabla u_h^{n-1}\|_{\Omega^n}^2 + \frac{\gamma_D \Delta t}{2h}\|u_h^n\|_{\partial\Omega^n}^2,$$

where $\gamma_D \ge 8/\epsilon$. By using the relation $2(a+b, a) = (a+b)^2 + a^2 - b^2$ for the first two terms in (3.18), we obtain that

$$\|u_h^n\|_{\Omega^n}^2 + \|u_h^n - u_h^{n-1}\|_{\Omega^n}^2 + \frac{\Delta t}{2}\|\nabla u_h^n\|_{\Omega^n}^2 + \frac{7\Delta t}{16}\|\nabla u_h^n + \nabla u_h^{n-1}\|_{\Omega^n}^2 + \frac{3\gamma_D \Delta t}{2h}\|u_h^n\|_{\partial\Omega^n}^2$$
$$+ 2\Delta t\gamma_g g_h^n(u_h^n, u_h^n) \le \|u_h^{n-1}\|_{\Omega^n}^2 + \frac{\Delta t}{2}\|\nabla u_h^{n-1}\|_{\Omega^n}^2 + 2\Delta t(f^{n-1/2}, u_h^n). \tag{3.19}$$

For $n > 1$, we bring the terms $\|u_h^{n-1}\|_{\Omega^n}$ and $\|\nabla u_h^{n-1}\|_{\Omega^n}$ to the domain Ω^{n-1}. By employing Lemmas 3.3 and 3.5, we have

$$\|u_h^{n-1}\|_{\Omega^n}^2 + \frac{\Delta t}{2}\|\nabla u_h^{n-1}\|_{\Omega^n}^2 \le \|u_h^{n-1}\|_{\Omega^{n-1}}^2 + c\Delta t\|u_h^{n-1}\|_{\partial\Omega^{n-1}}^2 + \frac{\Delta t}{2}\|\nabla u_h^{n-1}\|_{\Omega^{n-1}}^2$$
$$+ \left(\frac{\Delta t}{4} + c\Delta t^2\right)\|\nabla u_h^n + \nabla u_h^{n-1}\|_{\Omega^n}^2 + \left(\frac{1}{2} + c\Delta t\right)\|u_h^n - u_h^{n-1}\|_{\Omega^n}^2$$
$$+ c\Delta t g_h^n(u_h^n, u_h^n) + c\Delta t g_h^{n-1}(u_h^{n-1}, u_h^{n-1}). \tag{3.20}$$

Inserting (3.20) into (3.19) and using $2\Delta t(f^{n-1/2}, u_h^n)_{\Omega^n} \le \Delta t\left(\|f^{n-1/2}\|_{\Omega^n}^2 + \|u_h^n\|_{\Omega^n}^2\right)$ gives for sufficiently large γ_g

$$(1 - \Delta t)\|u_h^n\|_{\Omega^n}^2 + \frac{\Delta t}{2}\|\nabla u_h^n\|_{\Omega^n}^2 + \frac{1}{4}\|u_h^n - u_h^{n-1}\|_{\Omega^n}^2 + \frac{\Delta t}{8}\|\nabla u_h^n + \nabla u_h^{n-1}\|_{\Omega^n}^2$$
$$+ \frac{3\gamma_D \Delta t}{2h}\|u_h^n\|_{\partial\Omega^n}^2 + \Delta t\gamma_g g_h^n(u_h^n, u_h^n)$$
$$\le \|u_h^{n-1}\|_{\Omega^{n-1}}^2 + \frac{\Delta t}{2}\|\nabla u_h^{n-1}\|_{\Omega^{n-1}}^2 + c\Delta t\|u_h^{n-1}\|_{\partial\Omega^{n-1}}^2$$
$$+ c\Delta t g_h^{n-1}(u_h^{n-1}, u_h^{n-1}) + \Delta t\|f_h^{n-\frac{1}{2}}\|_{\Omega^n}^2. \tag{3.21}$$

For $n = 1$, we obtain from (3.19) and the stability of the extension E^1

$$(1 - \Delta t)\|u_h^1\|_{\Omega^1}^2 + \|u_h^1 - u_h^0\|_{\Omega^1}^2 + \frac{\Delta t}{2}\|\nabla u_h^1\|_{\Omega^1}^2 + \frac{3\Delta t}{8}\|\nabla u_h^1 + \nabla u_h^0\|_{\Omega^1}^2$$
$$+ \frac{3\gamma_D \Delta t}{2h}\|u_h^1\|_{\partial\Omega^1}^2 + 2\Delta t\gamma_g g_h^1(u_h^1, u_h^1)$$
$$\le \|E^1 u^0\|_{\Omega^1}^2 + \frac{\Delta t}{2}\|\nabla(E^1 u^0)\|_{\Omega^1}^2 + \Delta t\|f_h^{\frac{1}{2}}\|_{\Omega^1}^2$$
$$\le c\|u^0\|_{\Omega^0}^2 + c\Delta t\|\nabla u^0\|_{\Omega^0}^2 + \Delta t\|f_h^{\frac{1}{2}}\|_{\Omega^1}^2. \tag{3.22}$$

Taking the sum over $k = 1, 2, \ldots, n$, this yields for sufficiently large γ_g and γ_D

$$\|u_h^n\|_{\Omega^n}^2 + \Delta t \|\nabla u_h^n\|_{\Omega^n}^2 + \frac{\Delta t}{4} \sum_{k=1}^{n} \mathfrak{E}^k(u_h^k, u_h^{k-1})$$

$$\leq c\|u_h^0\|_{\Omega^0}^2 + c\Delta t \|\nabla u_h^0\|_{\Omega^0}^2 + 2t_n \|f\|_{\infty,0}^2 + c\Delta t \sum_{k=2}^{n} \|u_h^{k-1}\|_{\Omega^{k-1}}^2. \tag{3.23}$$

The statement follows by means of the discrete Gronwall lemma. □

Remark 3.7 (*Nitsche penalty term*) The definition of the Nitsche penalty term $\frac{\gamma_D}{h}(u_h^n, v_h)_{\partial\Omega^n}$ is motivated by the stability analysis. On one hand it is required to control the term $c\Delta t\|u_h^{n-1}\|_{\partial\Omega^{n-1}}$ (coming from the domain mismatch via Lemma 3.5) in (3.21). Moreover, if we would use the mixed penalty term $\frac{\gamma_D}{2h}(u_h^n + u_h^{n-1}, v_h)_{\partial\Omega^n}$ instead, testing with $v_h = 2\Delta t u_h^n$ would not be possible in Theorem 3.6, as

$$\frac{\gamma_D}{2h}(u_h^n + u_h^{n-1}, u_h^n)_{\partial\Omega^n} = \frac{\gamma_D}{4h}\left(\|u_h^n\|_{\partial\Omega^n}^2 + \|u_h^n + u_h^{n-1}\|_{\partial\Omega^n}^2 - \|u_h^{n-1}\|_{\partial\Omega^n}^2\right),$$

and the domain mismatch in the last term $\frac{\gamma_D}{4h}\|u_h^{n-1}\|_{\partial\Omega^n}$ can not be controlled by other terms in the variational formulation.

4 A Priori Error Analysis

In this section, we show an a priori error estimate for the discrete problem (2.7). We define the discretisation error as

$$e^n := E^n u^n - u_h^n, \quad n \geq 1, \tag{4.1}$$

where $u^n := u(t_n)$ is assumed to be at least in $H^2(\Omega^n)$ and E^n is the extension operator defined in Sect. 2.1.1. Within Ω^n the error e^n is precisely the discretisation error $u^n - u_h^n$. We use the extension operator to be able to use e^n also in parts of $\Omega_{h,\delta}^n$ that lie outside of Ω^n. Further regularity assumptions on u will be made below. The error is decomposed into an interpolation error η^n and a discrete error ξ_h^n terms defined by

$$\eta^n := E^n u^n - I_h^n E^n u^n, \qquad \xi_h^n := I_h^n E^n u^n - u_h^n, \tag{4.2}$$

where $I_h^n E^n u^n$ denotes the standard Lagrangian nodal interpolation of $E^n u^n$ on $\mathcal{T}_{h,\delta}^n$. For $n = 0$ we have, by definition of u_h^0, that $e^0 = u^0 - u_h^0 = 0$ in Ω^0 and thus, we also set $\eta^0 = \xi_h^0 = 0$. We will make use of the following standard interpolation estimates for $n \geq 1$

$$\|\eta^n\|_{H^l(\Omega)} \leq ch^{k-l}\|u^n\|_{H^k(\Omega)}, \quad \text{for } 0 \leq l \leq 1, \ 2 \leq k \leq m+1, \tag{4.3}$$

$$\|\eta^n\|_{H^l(\partial\Omega)} \leq ch^{k-l-1/2}\|u^n\|_{H^k(\Omega)}, \quad \text{for } 0 \leq l \leq 1, \ 2 \leq k \leq m+1. \tag{4.4}$$

4.1 Consistency Error

The exact solution $u \in H^1(\Omega(t))$ of the continuous problem (1.1) satisfies the following weak formulation:

$$(u_t, v)_{\Omega(t)} + a(u, v) = (f, v)_{\Omega(t)}, \quad t \in I_n \tag{4.5}$$

for $v \in H^1(\Omega(t))$ and the bilinear form

$$a(u, v) = (\nabla u, \nabla v)_{\Omega(t)} - (\partial_n u, v)_{\partial\Omega(t)}.$$

At time t_{n-1}, we have

$$(u_t(t_{n-1}), v)_{\Omega^{n-1}} + a^{n-1}(u^{n-1}, v) = (f^{n-1}, v)_{\Omega^{n-1}} \tag{4.6}$$

where

$$a^{n-1}(u^{n-1}, v) = (\nabla u^{n-1}, \nabla v)_{\Omega^{n-1}} - (\partial_n u^{n-1}, v)_{\partial\Omega^{n-1}}.$$

To estimate the consistency error, we will need an analogous equality for u^{n-1} on Ω^n instead of Ω^{n-1}. Therefore, we define $\tilde{u}$ as a smooth extension of the exact solution u to Q_δ^n which fulfills the properties given in (2.3)–(2.5). In the same way, we define a smooth extension of the source term f as follows:

$$\tilde{f}(t_{n-1}) = \tilde{u}_t(t_{n-1}) - \Delta\tilde{u}(t_{n-1}), \quad \text{on } \Omega_\delta^n. \tag{4.7}$$

It holds

$$\tilde{f}(t_{n-1}) = f(t_{n-1}) \quad \text{on } \Omega^{n-1}$$

However, as we have allowed an arbitrary smooth extension of f to Ω_δ^{n-1} in Sect. 2, this does not necessarily hold in $\Omega_\delta^{n-1} \setminus \Omega^{n-1}$. By using a test function $v_h \in V_h^{n,m}$, we get

$$(\tilde{u}_t^{n-1}, v_h)_{\Omega^n} + (\nabla\tilde{u}^{n-1}, \nabla v_h)_{\Omega^n} - (\partial_n\tilde{u}^{n-1}, v_h)_{\partial\Omega^n} = (\tilde{f}^{n-1}, v_h)_{\Omega^n}. \tag{4.8}$$

By adding the equations (4.5) and (4.8), we obtain

$$(u_t^n + \tilde{u}_t^{n-1}, v_h)_{\Omega^n} + (\nabla u^n + \nabla\tilde{u}^{n-1}, \nabla v_h)_{\Omega^n} - (\partial_n u^n + \partial_n\tilde{u}^{n-1}, v_h)_{\partial\Omega^n} = (f^n + \tilde{f}^{n-1}, v_h)_{\Omega^n}. \tag{4.9}$$

We note that the right-hand side in (4.9) differs from the discrete formulation (2.7) by $(\tilde{f}^{n-1} - f^{n-1}, v_h)_{\Omega^n \setminus \Omega^{n-1}}$. Hence, (4.9) can be rewritten as

$$\left(\frac{u_t^n + \tilde{u}_t^{n-1}}{2}, v_h\right)_{\Omega^n} + \frac{1}{2}a_h^n(u^n, v_h) + \frac{1}{2}a_h^{n-1}(\tilde{u}^{n-1}, v_h) = \frac{1}{2}(f^n + f^{n-1}, v_h)_{\Omega^n} + \frac{1}{2}\mathcal{E}_f^{n-1}(v_h), \tag{4.10}$$

where $\mathcal{E}_f^{n-1}(v_h)$ is given by

$$\mathcal{E}_f^{n-1}(v_h) = (\tilde{f}^{n-1} - f^{n-1}, v_h)_{\Omega^n \setminus \Omega^{n-1}}. \tag{4.11}$$

In the next lines, we will discuss a bound for the term $\mathcal{E}_f^{n-1}$.

Lemma 4.1 *Under the assumptions of Lemma 3.2, the error term $\mathcal{E}_f^{n-1}$ defined in (4.11) satisfies the following estimate for $v_h^n \in V_h^{n,m}$ and $u \in L^\infty(I, H^3(\Omega)) \cap W^{1,\infty}(I, H^1(\Omega))$:*

$$\Delta t \left|\mathcal{E}_f^{n-1}(v_h^n)\right| \le c\Delta t^5 \mathcal{R}_C(u)^2 + \frac{1}{32}\Big(\Delta t\|\nabla v_h^n + \nabla v_h^{n-1}\|_{\Omega^n}^2 + \|v_h^n - v_h^{n-1}\|_{\Omega^n}^2$$

$$+ \Delta t^2\|v_h^n\|_{\partial\Omega^n}^2 + \Delta t g_h^n(v_h^n, v_h^n) + \Delta t g_h^{n-1}(v_h^{n-1}, v_h^{n-1})\Big), \tag{4.12}$$

where $\mathcal{R}_C(u) = \|u\|_{\infty,3,I} + \|\partial_t u\|_{\infty,1,I}$.

Proof We apply Lemma 3.4 to $u = (f^{n-1} - \tilde{f}^{n-1})v_h^n$ for $p = 1$

$$
\begin{aligned}
\Delta t \big| (f^{n-1} - \tilde{f}^{n-1}, v_h^n)_{\Omega^n \setminus \Omega^{n-1}} \big| &\leq \Delta t \| (f^{n-1} - \tilde{f}^{n-1}) v_h^n \|_{L^1(\Omega^n \setminus \Omega^{n-1})} \\
&\leq c \Delta t^2 \| (f^{n-1} - \tilde{f}^{n-1}) v_h^n \|_{L^1(\partial \Omega^{n-1})} \\
&\quad + c \Delta t^3 \left\| \nabla \big[(f^{n-1} - \tilde{f}^{n-1}) v_h^n \big] \right\|_{L^1(\Omega^n \setminus \Omega^{n-1})}.
\end{aligned}
\tag{4.13}
$$

As $f^{n-1} = \tilde{f}^{n-1}$ on $\partial \Omega^{n-1}$, the first term in (4.13) vanishes. By definition of $\tilde{f}$ in (4.7) we can estimate further

$$
\begin{aligned}
\Delta t \big| (f^{n-1} - \tilde{f}^{n-1}, v_h^n)_{\Omega^n \setminus \Omega^{n-1}} \big| &\leq c \Delta t^3 \left[\| (f^{n-1} - \tilde{f}^{n-1}) \|_{\Omega^n \setminus \Omega^{n-1}} \| \nabla v_h^n \|_{\Omega^n \setminus \Omega^{n-1}} \right] \\
&\quad + c \Delta t^3 \left[\| \nabla (f^{n-1} - \tilde{f}^{n-1}) \|_{\Omega^n \setminus \Omega^{n-1}} \| v_h^n \|_{\Omega^n \setminus \Omega^{n-1}} \right] \\
&\leq c \Delta t^3 \mathcal{R}_C(u) \left[\| \nabla v_h^n \|_{\Omega^n \setminus \Omega^{n-1}} + \| v_h^n \|_{\Omega^n \setminus \Omega^{n-1}} \right].
\end{aligned}
\tag{4.14}
$$

Now, by employing Lemmas 3.3 and 3.5, we obtain

$$
\begin{aligned}
\| \nabla v_h^n \|_{\Omega^n \setminus \Omega^{n-1}}^2 + \| v_h^n \|_{\Omega^n \setminus \Omega^{n-1}}^2 &\leq \left(\frac{1}{2} + c \Delta t^2 \right) \| \nabla v_h^n + \nabla v_h^{n-1} \|_{\Omega^n \setminus \Omega^{n-1}}^2 \\
&\quad + \left(\frac{1}{\Delta t} + c \Delta t \right) \| v_h^n - v_h^{n-1} \|_{\Omega^n}^2 + c \Delta t \| v_h^n \|_{\partial \Omega^n}^2 + c g_h^n(v_h^n, v_h^n) + c g_h^{n-1}(v_h^{n-1}, v_h^{n-1}).
\end{aligned}
\tag{4.15}
$$

Inserting these estimates into (4.14) and using Young's inequality, we obtain

$$
\begin{aligned}
\Delta t \big| (f^{n-1} - \tilde{f}^{n-1}, v_h^n)_{\Omega^n \setminus \Omega^{n-1}} \big| &\leq c \Delta t^3 \mathcal{R}_C(u) \left[\| \nabla v_h^n \|_{\Omega^n \setminus \Omega^{n-1}} + \| v_h^n \|_{\Omega^n \setminus \Omega^{n-1}} \right] \\
&\leq c \Delta t^5 \mathcal{R}_C(u)^2 + \frac{1}{32} \Big(\Delta t \| \nabla v_h^n + \nabla v_h^{n-1} \|_{\Omega^n}^2 + \| v_h^n - v_h^{n-1} \|_{\Omega^n}^2 + \Delta t^2 \| v_h^n \|_{\partial \Omega^n}^2 \\
&\quad + \Delta t \gamma_g g_h^n(v_h^n, v_h^n) + \Delta t \gamma_g g_h^{n-1}(v_h^{n-1}, v_h^{n-1}) \Big).
\end{aligned}
\tag{4.16}
$$

$\square$

Now we are ready to estimate the consistency error related to the discrete problem (2.7). By subtracting (2.7) from (4.10), the global error term e^n satisfies the equality

$$
\begin{aligned}
\left(D_{\Delta t}^- e^n, v_h \right)_{\Omega^n} + \frac{1}{2} a_h^n(e^n, v_h) + \frac{1}{2} a_h^{n-1}(e^{n-1}, v_h) + \frac{\gamma_D}{h}(e^n, v_h)_{\partial \Omega^n} + \gamma_g g_h^n(e^n, v_h) \\
= \frac{1}{2} \mathcal{E}_f^{n-1}(v_h) + \mathcal{E}_c^n(v_h),
\end{aligned}
\tag{4.17}
$$

where the consistency error $\mathcal{E}_c^n(v_h)$ is given by

$$
\begin{aligned}
\mathcal{E}_c^n(v_h) = \underbrace{\left(D_{\Delta t}^- u^n - \partial_t(E^n u(t_{n-1/2})), v_h \right)_{\Omega^n}}_{I_1} \\
- \underbrace{\left(\frac{u_t(t_n) + \partial_t(E^n u(t_{n-1}))}{2} - \partial_t(E^n u(t_{n-1/2})), v_h \right)_{\Omega^n}}_{I_2} \\
+ \underbrace{\frac{\gamma_D}{h}(E^n u^n, v_h)_{\partial \Omega^n}}_{I_3} + \underbrace{\gamma_g g_h^n(E^n u^n, v_h)}_{I_4}.
\end{aligned}
\tag{4.18}
$$

The terms I_3 and I_4 vanish due to the homogeneous boundary condition and the regularity assumption on the exact solution $u^n \in H^2(\Omega^n)$ and its extension $E^n u^n \in H^2(\Omega_\delta^n)$. The remaining terms are estimated in the following lemma.

Lemma 4.2 *Let $u \in W^{3,\infty}(Q^n)$. Under Assumption 1, the consistency error for $v_h \in V_h^{n,m}$ is bounded by*

$$|\mathcal{E}_c^n(v_h^n)| \le c\Delta t^4 \|u\|_{W^{3,\infty}(Q^n)}^2 + \frac{1}{16}\|v_h^n\|_{\Omega^n}^2. \tag{4.19}$$

Proof First, we will show a bound for the term I_1. By following the argumentation in [60, Chapter 1], we have

$$\left|\left(\frac{u^n - E^n u^{n-1}}{\Delta t} - \partial_t E^n u(t_{n-1/2})\right)\right| \le \frac{1}{\Delta t}\left|\int_{t_{n-1/2}}^{t^n} \frac{(t_n - s)^2}{3!}\partial_t^3 E^n u(s)ds\right|$$
$$+ \frac{1}{\Delta t}\left|\int_{t^{n-1}}^{t_{n-1/2}} \frac{(s - t_{n-1})^2}{3!}\partial_t^3 E^n u(s)ds\right|$$
$$\le c\Delta t^2 \sup_{t\in[t_{n-1},t_n]} |\partial_t^3 E^n u(t)|.$$

Using the stability of the extension operator E^n given in (2.5) and the Cauchy-Schwarz inequality, we have

$$\left|\left(\frac{u^n - E^n u^{n-1}}{\Delta t} - \partial_t E^n u(t_{n-1/2}), v_h^n\right)_{\Omega^n}\right| \le c\Delta t^2 \|\partial_t^3 E^n u^n\|_{L^\infty(Q_\delta^n)}\|v_h^n\|_{\Omega^n}$$
$$\le c\Delta t^2 \|u\|_{W^{3,\infty}(Q^n)}\|v_h^n\|_{\Omega^n}. \tag{4.20}$$

A bound for the second term I_2 follows in a similar way, see also [60, Chapter 1]. The statement follows using Young's inequality. □

Remark 4.3 (Symmetric Nitsche formulation) If we would use a symmetric Nitsche formulation, i.e. including the term $-1/2(u_h^n + u_h^{n-1}, \partial_n v_h)_{\partial\Omega^n}$ in the discrete formulation (2.8), the term $-1/2(\tilde{u}^{n-1}, \partial_n v_h)_{\partial\Omega^n}$ would appear additionally on the right-hand side of (4.18). As $\tilde{u}^{n-1}$ is non-zero on the boundary $\partial\Omega^n$ in general, this term would dominate the consistency error, resulting in a significantly reduced order of convergence.

4.2 Interpolation Error

To derive an interpolation error estimate, we devise a discrete problem associated with the discrete error ξ_h^n. By definition of ξ_h^n (4.2) and using (4.17), we have for $v_h \in V_h^{n,m}$

$$\left(D_{\Delta t}^- \xi_h^n, v_h\right)_{\Omega^n} + \frac{1}{2}a_h^n(\xi_h^n, v_h) + \frac{1}{2}a_h^n(\xi_h^{n-1}, v_h) + \frac{\gamma_D}{h}(\xi_h^n, v_h)_{\partial\Omega^n}$$
$$+ \gamma_g g_h^n(\xi_h^n, v_h) = \frac{1}{2}\mathcal{E}_f^{n-1}(v_h) + \mathcal{E}_c^n(v_h) - \mathcal{E}_I^n(v_h), \tag{4.21}$$

where the interpolation error $\mathcal{E}_I^n(v_h)$ is given by

$$\mathcal{E}_I^n(v_h) = \left(D_{\Delta t}^- \eta^n, v_h\right)_{\Omega^n} + \frac{1}{2}a_h^n(\eta^n, v_h) + \frac{1}{2}a_h^n(\eta^{n-1}, v_h) + \frac{\gamma_D}{h}(\eta^n, v_h)_{\partial\Omega^n} + \gamma_g g_h^n(\eta^n, v_h). \tag{4.22}$$

Lemma 4.4 (Interpolation error) *Let $u \in L^\infty(I_n, H^{m+1}(\Omega(t)))$, $u_t \in L^\infty(I_n, H^m(\Omega(t)))$ and $v_h \in V_h^{n,m}$. Under Assumption 1, the interpolation error is bounded by*

$$|\mathcal{E}_I^n(v_h^n)| \le c\left(h^{2m} + \Delta t^2 h^{2m-2}\right)\mathcal{R}_I(u)^2 + \frac{1}{8}\|v_h^n\|_{\Omega^n}^2 + \frac{1}{32}\|\nabla v_h^n + \nabla v_h^{n-1}\|_{\Omega^n}^2$$
$$+ \frac{1}{32\Delta t}\|v_h^n - v_h^{n-1}\|_{\Omega^n}^2 + \frac{1}{16h}\|v_h^n\|_{\partial\Omega^n}^2 + \frac{1}{8}g_h^n(v_h^n, v_h^n), \tag{4.23}$$

where $\mathcal{R}_I(u) = \|u_t\|_{\infty,m} + \|u\|_{\infty,m+1}$ with the Bochner norms defined in (3.16).

Proof The first term in the interpolation error $\mathcal{E}_I^n(v_h)$ from (4.22) is estimated as follows:

$$
\begin{aligned}
\frac{1}{\Delta t}\left|\left(\eta^n - \eta^{n-1}, v_h^n\right)_{\Omega^n}\right| &\le \frac{1}{\Delta t}\|\eta^n - \eta^{n-1}\|_{\Omega^n}\|v_h^n\|_{\Omega^n} \\
&= \frac{1}{\Delta t}\left\|\int_{t_{n-1}}^{t_n}\eta_t(s)ds\right\|_{\Omega^n}\|v_h^n\|_{\Omega^n} \le h^m\|\partial_t E^n u\|_{\infty,m,I_n}\|v_h^n\|_{\Omega^n}.
\end{aligned}
$$
(4.24)

Using the stability of the extension (2.4), we obtain

$$
\frac{1}{\Delta t}\left|\left(\eta^n - \eta^{n-1}, v_h^n\right)_{\Omega^n}\right| \le c\,h^m\left(\|u_t\|_{\infty,m} + \|u\|_{\infty,m+1}\right)\|v_h^n\|_{\Omega^n}. \tag{4.25}
$$

Next, we use interpolation estimates (4.3) and (4.4) in combination with (2.3) to deduce for $k \in \{n-1, n\}$ that

$$
\begin{aligned}
\frac{1}{2}\left|a_h^n(\eta^k, v_h^n)\right| &\le \frac{1}{2}\|\nabla\eta^k\|_{\Omega^n}\|\nabla v_h^n\|_{\Omega^n} + \|\partial_n\eta^k\|_{\partial\Omega^n}\|v_h^n\|_{\partial\Omega^n} \\
&\le ch^m\|u^k\|_{H^{m+1}(\Omega^k)}\|\nabla v_h^n\|_{\Omega^n} + ch^{m-1/2}\|u^k\|_{H^{m+1}(\Omega^k)}\|v_h^n\|_{\partial\Omega^n}.
\end{aligned}
$$
(4.26)

Using that, by an inverse inequality

$$
\begin{aligned}
\|\nabla v_h^n\|_{\Omega^n} &\le \frac{1}{2}\|\nabla v_h^n + \nabla v_h^{n-1}\|_{\Omega^n} + \frac{1}{2}\|\nabla v_h^n - \nabla v_h^{n-1}\|_{\Omega^n} \\
&\le \frac{1}{2}\|\nabla v_h^n + \nabla v_h^{n-1}\|_{\Omega^n} + \frac{c}{h}\|v_h^n - v_h^{n-1}\|_{\Omega^n}
\end{aligned}
$$

we obtain further

$$
\begin{aligned}
\frac{1}{2}\left|a_h^n(\eta^k, v_h^n)\right| &\le c\,h^m\|u^k\|_{H^{m+1}(\Omega^k)}\left(\frac{1}{2}\|\nabla v_h^n + \nabla v_h^{n-1}\|_{\Omega^n} + \frac{1}{h^{1/2}}\|v_h^n\|_{\partial\Omega^n}\right) \\
&\quad + ch^{m-1}\|u^k\|_{H^{m+1}\Omega^k)}\|v_h^n - v_h^{n-1}\|_{\Omega^n}.
\end{aligned}
$$
(4.27)

For the Nitsche penalty term, we have

$$
\left|\frac{\gamma_D}{h}(\eta^n, v_h^n)_{\partial\Omega^n}\right| \le c\frac{\gamma_D}{h}\|\eta^n\|_{\partial\Omega^n}\|v_h^n\|_{\partial\Omega^n} \le ch^m\|u^n\|_{H^{m+1}(\Omega^n)}\frac{1}{h^{1/2}}\|v_h^n\|_{\partial\Omega^n}. \tag{4.28}
$$

Finally, the ghost-penalty term is approximated by using $g_h^n(\eta^n, v_h^n) \le g_h^n(\eta^n, \eta^n)^{1/2} g_h^n(v_h^n, v_h^n)^{1/2}$ and an interpolation estimate

$$
\left|\gamma_g g_h^n(\eta^n, v_h^n)\right| \le ch^m\|u^n\|_{H^{m+1}(\Omega^n)}g_h^n(v_h^n, v_h^n)^{1/2}. \tag{4.29}
$$

The statement (4.23) follows by combining estimates (4.25)–(4.29) and using Young's inequality. $\qquad\square$

4.3 Convergence Estimate

Lemma 4.5 (Discrete error) *Let* $u \in L^\infty(I_n, H^{m+1}(\Omega(t))) \cap W^{1,\infty}(I_n, H^m(\Omega(t)) \cap W^{3,\infty}(Q)$ *be the solution of (1.1) and* $\{u_h^k\}_{k=1}^n$ *the discrete solution of (2.7), respectively. Under Assumptions 1 and 2, the discrete error term* ξ_h^n *satisfies for* γ_g, γ_D *sufficiently large*

$$
\|\xi_h^n\|_{\Omega^n}^2 + \Delta t\|\nabla\xi_h^n\|_{\Omega^n}^2 + \Delta t\sum_{k=1}^n \mathfrak{E}^k(\xi_h^k, \xi_h^{k-1}) \le \exp(c_{T\,4.5}t_n)\left(\Delta t^4 + \Delta t\,h^{2m-2} + h^{2m}\right)\mathcal{R}(u)^2,
$$
(4.30)

where $\mathcal{R}(u) = \mathcal{R}_C(u) + \mathcal{R}_I(u) + \|u\|_{W^{3,\infty}(Q)}$, *with* $\mathcal{R}_C$ *and* $\mathcal{R}_I$ *specified in Lemma 4.1 and 4.4, respectively.*

Proof By taking $v_h = 2\Delta t \xi_h^k$ in (4.21) and using the argumentation from the stability proof (Theorem 3.6), see (3.21), we obtain that

$$\|\xi_h^k\|_{\Omega^k}^2 + \frac{1}{4}\|\xi_h^k - \xi_h^{k-1}\|_{\Omega^k}^2 + \frac{\Delta t}{2}\|\nabla\xi_h^k\|_{\Omega^k}^2 + \frac{\Delta t}{8}\|\nabla\xi_h^k + \nabla\xi_h^{k-1}\|_{\Omega^k}^2 + \frac{3\gamma_D\Delta t}{2h}\|\xi_h^k\|_{\partial\Omega^k}^2$$
$$+2\Delta t\gamma_g g_h(\xi_h^k, \xi_h^k) \le \|\xi_h^{k-1}\|_{\Omega^{k-1}}^2 + \frac{\Delta t}{2}\|\nabla\xi_h^{k-1}\|_{\Omega^{k-1}}^2 + c\Delta t\|\xi_h^{k-1}\|_{\partial\Omega^{k-1}}^2$$
$$+c\Delta t g_h^{k-1}(\xi_h^{k-1}, \xi_h^{k-1}) + 2\Delta t\left(|\mathcal{E}_f^{k-1}(\xi_h^k)| + |\mathcal{E}_c^k(\xi_h^k)| + |\mathcal{E}_I^k(\xi_h^k)|\right).$$
(4.31)

By combining results from Lemmas 4.1, 4.2 and 4.4 we have

$$2\Delta t\left(|\mathcal{E}_f^{k-1}(\xi_h^k)| + |\mathcal{E}_c^k(\xi_h^k)| + |\mathcal{E}_I^k(\xi_h^k)|\right) \le c\Delta t\left(\Delta t^4 + \Delta t\, h^{2m-2} + h^{2m}\right)\mathcal{R}(u)$$
$$+ \frac{\Delta t}{4}\|\xi_h^k\|_{\Omega^k}^2 + \frac{\Delta t}{16}\|\nabla\xi_h^k + \nabla\xi_h^{k-1}\|_{\Omega^k}^2$$
$$+ \frac{1}{16}\|\xi_h^k - \xi_h^{k-1}\|_{\Omega^k}^2 + \frac{\Delta t}{8h}\|\xi_h^k\|_{\partial\Omega^k}^2$$
$$+ c\Delta t g_h^k(\xi_h^k, \xi_h^k) + c\Delta t g_h^{k-1}(\xi_h^{k-1}, \xi_h^{k-1}).$$
(4.32)

Inserting (4.32) into (4.31) and absorbing terms into the left-hand side yields for $k > 1$ and γ_D, γ_g sufficiently large

$$\left(1 - \frac{\Delta t}{4}\right)\|\xi_h^k\|_{\Omega^k}^2 + \frac{3}{16}\|\xi_h^k - \xi_h^{k-1}\|_{\Omega^k}^2 + \frac{\Delta t}{4}\|\nabla\xi_h^k\|_{\Omega^k}^2 + \frac{\Delta t}{16}\|\nabla\xi_h^k + \nabla\xi_h^{k-1}\|_{\Omega^k}^2$$
$$+ \frac{\gamma_D\Delta t}{h}\|\xi_h^k\|_{\partial\Omega^k}^2 + \Delta t\gamma_g g_h(\xi_h^k, \xi_h^k) \le \|\xi_h^{k-1}\|_{\Omega^{k-1}}^2 + \frac{\Delta t}{2}\|\nabla\xi_h^{k-1}\|_{\Omega^{k-1}}^2 + c\Delta t\|\xi_h^{k-1}\|_{\partial\Omega^{k-1}}^2$$
$$+ c\Delta t g_h^{k-1}(\xi_h^{k-1}, \xi_h^{k-1}) + c\Delta t\left(\Delta t^4 + \Delta t\, h^{2m-2} + h^{2m}\right)\mathcal{R}(u).$$
(4.33)

As $\xi_h^0 = 0$, we obtain for $k = 1$

$$\left(1 - \frac{\Delta t}{4}\right)\|\xi_h^1\|_{\Omega^1}^2 + \frac{3}{16}\|\xi_h^1 - \xi_h^0\|_{\Omega^1}^2 + \frac{\Delta t}{2}\|\nabla\xi_h^1\|_{\Omega^1}^2 + \frac{\Delta t}{16}\|\nabla\xi_h^1 + \nabla\xi_h^0\|_{\Omega^1}^2$$
$$+ \frac{\gamma_D\Delta t}{h}\|\xi_h^1\|_{\partial\Omega^1}^2 + \Delta t\gamma_g g_h^1(\xi_h^1, \xi_h^1) \le c\Delta t\left(\Delta t^4 + h^{2m}\right)\mathcal{R}(u).$$

Now, summing over $k = 1, 2, \ldots, n$, we deduce that

$$\|\xi_h^n\|_{\Omega^n}^2 + \Delta t\|\nabla\xi_h^n\|_{\Omega^n}^2 + \Delta t\sum_{k=1}^n \mathfrak{E}^k(\xi_h^k, \xi_h^{k-1})$$
$$\le c\, t_n\left(\Delta t^4 + \Delta t\, h^{2m-2} + h^{2m}\right)\mathcal{R}(u) + c\Delta t\sum_{k=2}^n \|\xi_h^{k-1}\|_{\Omega^{k-1}}^2.$$
(4.34)

Finally, we use the discrete Gronwall lemma to conclude the result. This completes the proof. □

Theorem 4.6 (Global error) *Under the assumptions made in Lemma 4.5, the global error $e^k = E^k u^k - u_h^k$, $k = 1, ..., n$ satisfies*

$$\|e^n\|_{\Omega^n}^2 + \Delta t\|\nabla e^n\|_{\Omega^n}^2 + \Delta t\sum_{k=1}^n \mathfrak{E}^k(e^k, e^{k-1}) \le \exp(c_{T\,4.6}t_n)\left(\Delta t^4 + \Delta t\, h^{2m-2} + h^{2m}\right)\mathcal{R}(u)^2,$$
(4.35)

where $\mathcal{R}(u)$ is defined in Lemma 4.5.

Proof Using the interpolation error estimates (4.3), (4.4) and (4.25), we deduce that

$$\|\eta_h^n\|_{\Omega^n}^2 + \Delta t \|\nabla \eta_h^n\|_{\Omega^n}^2 + \Delta t \sum_{k=1}^{n} \mathfrak{E}^k(\eta_h^k, \eta_h^{k-1}) \leq c\, h^{2m} \mathcal{R}_I(u)^2. \tag{4.36}$$

In combination with Lemma 4.5, this proves (4.35). □

Remark 4.7 Under the CFL condition $\Delta t \leq c_{\mathrm{CFL}} h^{3/2}$ assumed in the stability estimate, we obtain an error estimate of order $\mathcal{O}(\Delta t^2 + h^{m-1/4})$ (after taking the square root in (4.35)). This is suboptimal by $\mathcal{O}(h^{1/4})$ compared to the estimate on a stationary domain. The optimal error estimate $\mathcal{O}(\Delta t^2 + h^m)$ results under the stronger condition $\Delta t \leq ch^2$.

5 Numerical Results

In this section, we show numerical results in two and three space dimensions to verify the theoretical findings and the practical behaviour of the numerical method. All the numerical experiments have been obtained using the CutFEM library [8], which is based on FEniCS [1].

To verify the theoretical results, we will analyse the error terms $e^k = u^k - u_h^k$, $k = 1, ..., n$ in the following norms

$$\|e^n\|_{L^2(\Omega^n)}, \ \|e\|_{L^2(L^2)} = \left(\Delta t \sum_{k=1}^{n} \|e^k\|_{L^2(\Omega^k)}^2 \right)^{1/2}, \ \|e\|_{L^2(H_{av}^1)}$$

$$= \left(\Delta t \sum_{k=1}^{n} \|\nabla e^k + \nabla e^{k-1}\|_{\Omega^k}^2 \right)^{1/2}.$$

Given the stronger CFL condition $\Delta t \leq ch^2$, Theorem 4.6 guarantees second-order convergence in time and convergence of order m in space in the L^2-norm at the end time $\|e^n\|_{L^2(\Omega^n)}$ and in the averaged $L^2(H^1)$-norm $\|e\|_{L^2(H_{av}^1)}$.

5.1 2D Example with Exponential Decay

Example 5.1 We consider a circle travelling with constant velocity $w = (1, 0)$ towards the right. The domain is given by

$$\Omega(t) = \{(x, y) : (x - 0.5 - t)^2 + (y - 0.5)^2 \leq 0.9\}$$

in the time interval $I = [0, 0.1]$. The data of the model example is chosen in such a way that the exact solution is

$$u(x, y, t) = \exp(-4\pi^2 t) \cos(2\pi x) \cos(2\pi y).$$

An illustration of the numerical solution is given in Fig. 3. As background domain D, we use the unit square, i.e. $D = [0, 1]^2$. The background triangulations $\mathcal{T}_h$ are created by a uniform subdivision of the unit square into triangles and successive refinement. For each time step n, the active triangulation $\mathcal{T}_{h,\delta}^n$ is then extracted from $\mathcal{T}_h$, as described in Sect. 2. We use $\delta = 4\Delta t$.

Estimated orders of convergence We will show results for different time-step sizes $\Delta t_i = 1/50 \cdot 2^{-i}$, $i = 0, ..., 4$ and mesh sizes $h_j = 1/32 \cdot 2^{-j}$, $j = 0, ..., 3$. From the computed
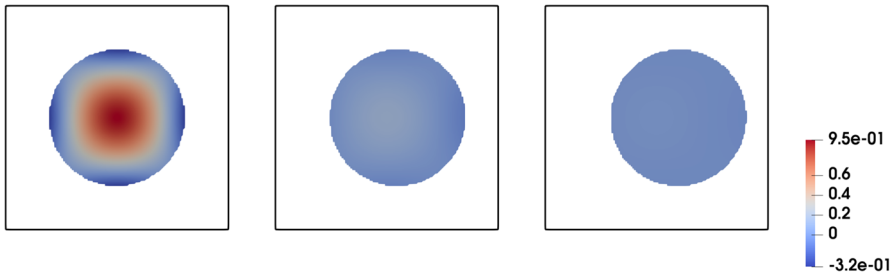
Fig. 3 Illustration of the numerical solution u of Example 5.1 at $t = 0$ (left), $t = 0.05$ (center) and $t = 0.1$ (right)

errors, we will estimate the temporal and spatial order of convergence. Therefore, we assume that the total error can be decomposed into a temporal and a spatial component as follows

$$g(\Delta t, h) = g_{\Delta t}(\Delta t) + g_h(h) = c_{\Delta t}\Delta t^{eoc_{\Delta t}} + c_h h^{eoc_h}$$

with constants $c_{\Delta t}, c_h$ and estimated orders of convergence $eoc_{\Delta t}$, eoc_h. For a fixed mesh size h_j, this relation becomes

$$g(\Delta t, \cdot) = g_{h_j} + c_{\Delta t}\Delta t^{eoc_{\Delta t}} \tag{5.1}$$

with a fixed spatial error part g_{h_j}. We will use (5.1) to estimate the order of convergence in time $eoc_{\Delta t}$ by means of a least-squares fit of all available error values for a fixed h_j to find the three parameters g_{h_j}, $c_{\Delta t}$ and $eoc_{\Delta t}$. Analogously, we estimate the spatial order of convergence eoc_h by a least-squares fit of the function

$$g(\cdot, h) = g_{\Delta t_i} + c_h h^{eoc_h} \tag{5.2}$$

against all available error values for a fixed time-step size Δt_i.

Moreover, we will also compute estimated orders of convergence for the "diagonal values", which correspond to fixing $\Delta t = \bar{c}h$ for $\bar{c} \in \{32/50, 32/100, 32/200\}$. Here we fit the two parameters $c_{\Delta t,h}$ and $eoc_{\Delta t,h}$ of the function

$$g(\bar{c}h, h) = c_{\Delta t,h}h^{eoc_{\Delta t,h}}. \tag{5.3}$$

against the computed error values. Finally, we will also use (5.3) to estimate $eoc_{\Delta t,h}$ by means of two values for $\Delta t = \bar{c}h$ and $\frac{\Delta t}{2} = \bar{c}\frac{h}{2}$

$$\widetilde{eoc}_{\Delta t,h} := \log_2\left(\frac{g(\bar{c}h, h)}{g(\bar{c}h/2, h/2)}\right). \tag{5.4}$$

5.1.1 P_1 Finite Elements

Firstly, we consider P_1 finite elements. We choose the numerical parameters as $\gamma_D = 1$ and $\gamma_g = 10^{-3}$. The errors in the L^2-norm at the end time, the $L^2(L^2)$-norm and the $L^2(H^1_{av})$-norm are shown in Table 1 (a)–(c) for different Δt and h. The estimated orders of convergence are shown, if the asymptotic standard error (computed by gnuplot [64]) was below 20%; otherwise we draw a '-'.

We observe estimated spatial convergence orders close to two in the L^2-norms and close to one in the $L^2(H^1_{av})$-norm. Note that Theorem 4.6 guarantees only first-order convergence

Table 1 (a)–(c): $L^2(T)$, $L^2(L^2)$ and $L^2(H^1_{av})$-norm errors for P_1 finite elements applied to Example 5.1

| (a) End-time error $\|e^n\|_{L^2(\Omega^n)}$ | | | | | | |
$h \downarrow / \Delta t \rightarrow$ 1/50	1/100	1/200	1/400	1/800	**eoc$_{\Delta t}$**
1/32 1.93e–03	5.40e–04	3.14e–04	2.78e–04	2.68e–04	**2.62**
1/64 1.21e–03	2.77e–04	1.08e–04	7.84e–05	7.17e–05	**2.46**
1/128 8.88e–04	1.96e–04	4.95e–05	2.54e–05	1.96e–05	**2.29**
1/256 7.78e–04	1.57e–04	3.18e–05	1.15e–05	6.18e–06	**2.35**
eoc$_h$ **1.26**	**1.55**	**1.80**	**1.91**	**1.92**	
eoc$_{\Delta t,h}$			**2.79**	**2.30**	

| (b) Error $\|e\|_{L^2(L^2)}$ | | | | | | |
$h \downarrow / \Delta t \rightarrow$ 1/50	1/100	1/200	1/400	1/800	**eoc$_{\Delta t}$**
1/32 1.44e–03	8.42e–04	7.12e–04	6.87e–04	6.83e–04	**2.25**
1/64 9.69e–04	3.62e–04	2.21e–04	1.89e–04	1.82e–04	**2.11**
1/128 8.35e–04	2.37e–04	9.13e–05	5.72e–05	4.89e–05	**2.04**
1/256 7.97e–04	2.01e–04	5.75e–05	2.30e–05	1.45e–05	**2.05**
eoc$_h$ **1.81**	**1.91**	**1.92**	**1.92**	**1.92**	
eoc$_{\Delta t,h}$			**1.99**	**1.93**	

| (c) Error $\|e\|_{L^2(H^1_{av})}$ | | | | | | |
$h \downarrow / \Delta t \rightarrow$ 1/50	1/100	1/200	1/400	1/800	**eoc$_{\Delta t}$**
1/32 4.77e–02	4.53e–02	4.50e–02	4.49e–02	4.49e–02	**2.83**
1/64 2.64e–02	2.36e–02	2.33e–02	2.33e–02	2.33e–02	**3.33**
1/128 1.65e–02	1.23e–02	1.19e–02	1.19e–02	1.19e–02	**3.32**
1/256 1.26e–02	6.72e–03	6.06e–03	6.01e–03	6.00e–03	**3.21**
eoc$_h$ **1.17**	**0.96**	**0.93**	**0.93**	**0.93**	
eoc$_{\Delta t,h}$			**1.00**	**0.96**	

| (d) Diagonal errors for $h = \bar{c}\Delta t$ | | | | | |
$h = \bar{c}\Delta t \downarrow$ $\|e^n\|_{L^2(\Omega^n)}$	eõc$_{h,\Delta t}$	$\|e\|_{L^2(L^2)}$	eõc$_{h,\Delta t}$	$\|e\|_{L^2(H^1_{av})}$	eõc$_{h,\Delta t}$
1/100 5.40e–04	–	8.42e–04	–	4.53e–02	–
1/200 1.08e–04	2.32	2.21e–04	1.93	2.33e–02	0.96
1/400 2.54e–05	2.09	5.72e–05	1.95	1.19e–02	0.97
1/800 6.18e–06	2.04	1.45e–05	1.98	6.00e–03	0.99

The estimated orders of convergence are computed according to (5.1)–(5.3). The diagonal orders are computed from the underlined error values. (d): Estimated order of convergence eõc$_{h,\Delta t}$ for $\Delta t = \bar{c}h \rightarrow 0$ obtained by (5.4) by comparing two consecutive error values

in space (under the stronger CFL condition $\Delta t \leq ch^2$). We expect, however, that using a duality argument second-order convergence in space could be shown in the $L^2(L^2)$-norm, as in [12].

The estimated temporal orders of convergence are close to two or larger in the L^2-norms. This is in agreement with Theorem 4.6. In the $L^2(H^1_{av})$-norm the estimated eoc$_{\Delta t}$ seems to be even larger than three. This has to be read carefully, however, as the spatial error part clearly dominates the overall error in this case.

Finally, the diagonal orders are around two in the $L^2(L^2)$-norm and even slightly higher in the L^2-norm at the end time. In the $L^2(H_{av})$-norm the spatial part is dominant and we obtain $eoc_{\Delta t,h}$ close the one, in agreement with Theorem 4.6. In Table 1(d), we show the diagonal orders obtained by formula (5.4) by comparing two consecutive values. The results are similar, with the orders for smaller $\Delta t = \bar{c}h$ being even closer to 2 resp. 1.

We remark that the CFL condition $\Delta t \leq c_{CFL}h^{3/2}$ is by far violated for the finer meshes and coarser time steps. In the present setting with perfectly uniform grids and P_1-finite elements, we expect that both constants c_0 and c_{inv} entering c_{CFL} are (relatively) close to one. For the largest Δt and the smallest h considered, we have, e.g., $\Delta t = 1/50 \gg 1/4096 = (1/256)^{3/2} = h^{3/2}$. Nevertheless, we did not observe any instabilities in the computations and optimal convergence orders are obtained.

5.1.2 P_2 Finite Elements

Next, we consider Example 5.1 with P_2 finite elements. We increase the Nitsche parameter to $\gamma_D = 10$, as for polynomials of higher degree a larger Nitsche parameter is required, see e.g. [44]. The ghost-penalty parameter γ_g is still chosen as 10^{-3}, but now, according to (2.9), second derivatives are included in the ghost-penalty term. The L^2-norm errors at the end time, the $L^2(L^2)$- and the $L^2(H^1_{av})$-norm errors are shown in Table 2 (a)–(c).

Firstly, we observe that the absolute values of the errors are significantly smaller compared to P_1 finite elements. The spatial orders of convergence are close to two in all norms for smaller Δt. We note that in Theorem 4.6 second order in space has been shown for the end-time L^2-norm and the $L^2(H^1_{av})$-norm (under the stronger CFL condition $\Delta t \leq ch^2$). Using a duality argument, one could even hope for convergence order three in the $L^2(L^2)$-norm. We need to consider, however, that for these results the quadrature error related to a curved boundary has not been taken into account. In the CutFEM library used here, the geometry is approximated linearly in the set-up of the quadrature rule, see [8]. This can lead to a reduced order of convergence, namely order 1.5 in the H^1-norms and 2 in the L^2-norms, see [13] for results for a CutFEM approach applied to an elliptic problem on curved domains. This reduction can also be observed in the L^2-norm errors in the example considered here.

The estimated temporal orders of convergence are again close to two in the L^2-norms, which confirm the estimates in Theorem 4.6. In the $L^2(H^1_{av})$-norm the error is still clearly dominated by the spatial part for $h \geq \frac{1}{64}$. This changes, however, on the finer levels, where the temporal part gets dominant and the $eoc_{\Delta t}$ is very close to two, in agreement with Theorem 4.6.

The spatial and temporal convergence orders are confirmed by the "diagonal" orders, which are close to two for the L^2-norms and slightly below 2 in the $L^2(H^1_{av})$-norm. In all cases, the orders are equal to or larger than the expected orders for a linear interface approximation. The observations are confirmed in Table 2 (d), where the order of convergence is estimated by means of two consecutive error values by (5.4).

As in the case of P_1 finite elements the CFL condition is severely violated for the finer meshes and coarser time steps. Again, we did not observe any stability issues or reduced convergence orders.

Table 2 (a)–(c): $L^2(T)$, $L^2(L^2)$ and $L^2(H^1_{av})$-norm errors for P_2 finite elements applied to Example 5.1. (d): Estimated order of convergence $e\tilde{o}c_{h,\Delta t}$ for $\Delta t = \bar{c}h \to 0$ obtained by (5.4) by comparing two consecutive error values

(a) End-time error $\|e^n\|_{L^2(\Omega^n)}$

$h \downarrow / \Delta t \to$	1/100	1/200	1/400	1/800	1/1600	**eoc$_{\Delta t}$**
1/32	1.16e–04	3.09e–05	1.08e–05	5.80e–06	4.66e–06	**2.06**
1/64	1.17e–04	2.66e–05	7.33e–06	2.78e–06	1.44e–06	**2.18**
1/128	1.11e–04	2.43e–05	6.23e–06	1.76e–06	6.78e–07	**2.22**
1/256	1.12e–04	2.31e–05	5.78e–06	1.54e–06	4.36e–07	**2.29**
eoc$_h$	**–**	**0.91**	**1.60**	**1.68**	**2.01**	
eoc$_{\Delta t,h}$				**2.12**	**2.08**	

(b) Error $\|e\|_{L^2(L^2)}$

$h \downarrow / \Delta t \to$	1/100	1/200	1/400	1/800	1/1 600	**eoc$_{\Delta t}$**
1/32	1.89e–04	5.35e–05	2.13e–05	1.27e–05	1.10e–05	**2.04**
1/64	1.84e–04	4.66e–05	1.36e–05	5.09e–06	3.16e–06	**2.03**
1/128	1.82e–04	4.50e–05	1.16e–05	3.32e–06	1.28e–06	**2.03**
1/256	1.82e–04	4.45e–05	1.12e–05	2.88e–06	8.32e–07	**2.03**
eoc$_h$	**1.72**	**2.00**	**1.99**	**2.09**	**2.05**	
eoc$_{\Delta t,h}$				**2.02**	**1.98**	

(c) Error $\|e\|_{L^2(H^1_{av})}$

$h \downarrow / \Delta t \to$	1/100	1/200	1/400	1/800	1/1 600	**eoc$_{\Delta t}$**
1/32	3.42e–03	2.25e–03	2.17e–03	2.17e–03	2.17e–03	**3.88**
1/64	2.81e–03	9.11e–04	6.22e–04	6.03e–04	6.03e–04	**2.82**
1/128	2.80e–03	7.26e–04	2.45e–04	1.77e–04	1.72e–04	**2.22**
1/256	2.81e–03	7.14e–04	1.87e–04	6.84e–05	5.30e–05	**2.03**
eoc$_h$	**–**	**2.91**	**2.11**	**1.89**	**1.86**	
eoc$_{\Delta t,h}$				**1.90**	**1.85**	

(d) Diagonal errors for $h = \bar{c}\Delta t$

$h = \bar{c}\Delta t \downarrow$	$\|e^n\|_{L^2(\Omega^n)}$	$e\tilde{o}c_{h,\Delta t}$	$\|e\|_{L^2(L^2)}$	$e\tilde{o}c_{h,\Delta t}$	$\|e\|_{L^2(H^1_{av})}$	$e\tilde{o}c_{h,\Delta t}$
1/200	3.09e–05	–	5.35e–05	–	2.25e–03	–
1/400	7.33e–06	2.06	1.36e–05	1.98	6.22e–04	1.85
1/800	1.76e–06	2.06	3.32e–06	2.03	1.77e–04	1.81
1/1600	4.36e–07	2.01	8.32e–07	2.00	5.30e–05	1.74

5.2 2D Example with Monotonically Increasing Solution

In order to show that the numerical convergence orders obtained in the previous example do not depend on the fact that the solution decays exponentially in time, we consider a second example with a monotonically increasing solution u.

Example 5.2 We consider the moving domain $\Omega(t)$ from Example 5.1 and again $I = [0, 0.1]$. However, the data is now chosen in such a way that the exact solution is

$$u(x, y, t) = \sin(\pi t)\cos(2\pi x)\cos(2\pi y),$$

Table 3 Estimated order of convergence $e\tilde{o}c_{h,\Delta t}$ in Example 5.2 for $\Delta t = \bar{c}h \to 0$ for P_1 and P_2 finite elements. The values have been obtained by (5.4) by comparing two consecutive error values

| (a) Diagonal errors for $h = \bar{c}\Delta t$ and P_1 finite elements | | | | | |
$h = \bar{c}\Delta t \downarrow$	$\|e^n\|_{L^2(\Omega^n)}$	$e\tilde{o}c_{h,\Delta t}$	$\|e\|_{L^2(L^2)}$	$e\tilde{o}c_{h,\Delta t}$	$\|e\|_{L^2(H^1_{av})}$	$e\tilde{o}c_{h,\Delta t}$
1/100	5.21e−03	–	9.96e−04	–	2.73e−02	–
1/200	1.53e−03	1.78	2.88e−04	1.79	1.20e−02	1.18
1/400	4.07e−04	1.91	7.73e−05	1.90	5.56e−03	1.11
1/800	1.07e−04	1.93	2.06e−05	1.91	2.66e−03	1.06
(b) Diagonal errors for $h = \bar{c}\Delta t$ and P_2 finite elements					
$h = \bar{c}\Delta t \downarrow$	$\|e^n\|_{L^2(\Omega^n)}$	$e\tilde{o}c_{h,\Delta t}$	$\|e\|_{L^2(L^2)}$	$e\tilde{o}c_{h,\Delta t}$	$\|e\|_{L^2(H^1_{av})}$	$e\tilde{o}c_{h,\Delta t}$
1/200	3.71e−05	–	6.45e−06	–	1.09e−03	–
1/400	9.46e−06	1.97	1.61e−06	2.00	3.06e−04	1.83
1/800	2.46e−06	1.96	4.12e−07	1.97	8.84e−05	1.79
1/1600	6.04e−07	2.02	1.03e−07	2.00	2.68e−05	1.72

i.e. it is monotonically increasing in time within I.

As in the previous example, we consider P_1 and P_2 finite elements. In both cases, all numerical parameters are chosen exactly as in Sect. 5.1.1.

In Table 3, we show errors obtained for a fixed ratio $\Delta t = \bar{c}h$ ($\bar{c} = 32/100$ for $m = 1$ and $\bar{c} = 32/200$ for $m = 2$), and corresponding estimates for the "diagonal" orders of convergence $eoc_{\Delta t,h}$ obtained by formula (5.4). In both cases the results are very similar to the previous example: For P_1 finite elements, we observe quadratic convergence in the L^2-norms and linear convergence in the $L^2(H^1_{av})$ norm, as expected. For P_2 elements, we obtain second-order convergence in the L^2-norms and slightly reduced orders in [1.72, 1.83] in the $L^2(H^1_{av})$ norm. The latter can again be explained by the fact that the interface is only approximated linearly in our computations, which can reduce the spatial order of convergence down to 1.5. As in the previous example, we did not observe any stability issues, although the CFL condition is severely violated on the finer meshes for coarser time steps.

5.3 3D Example

Example 5.3 We consider a 3-dimensional rectangular channel with a moving upper and lower wall in the time interval $I = [0, 1]$, inspired by a pump. The moving domain is given by

$$\Omega(t) = (0, 4) \times (-1 + 0.1 \sin t, 1 - 0.1 \sin t) \times (-1, 1).$$

The source term and boundary data are chosen in such a way that the exact solution of the model problem (1.1) is

$$u(x, y, z, t) = \exp(-t)\left((1 - 0.1 \sin t)^2 - y^2\right).$$

As background domain D, we use the box $[0, 4] \times [-1.1, 1.1] \times [-1, 1]$. The background triangulations $\mathcal{T}_h$ are created by uniform subdivisions of D into tetrahedra and successive refinement. We use again $\delta = 4\Delta t$ and choose $\gamma_g = 0.1$ for P_1 and $\gamma_g = 1$ for P_2 finite elements, respectively and $\gamma_D = 10$ in both cases. We note that in this example the quadrature
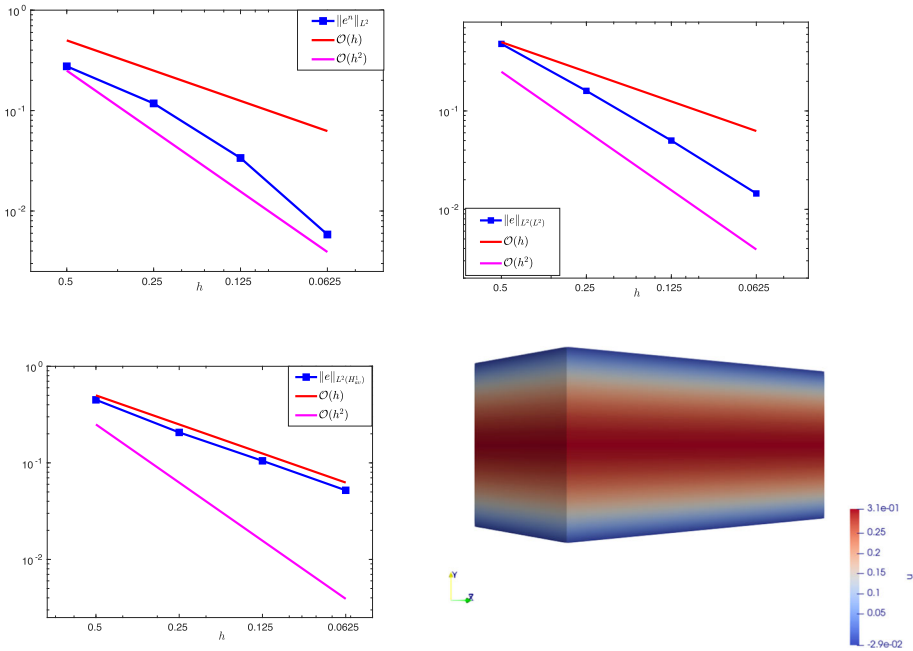
Fig. 4 Errors for example 5.2 (3d) for P_1 finite elements under simultaneous refinement in space and time ($\Delta t = h/10$) for P_1 finite elements. Top left: L^2-norm at the end time. Top right: $L^2(L^2)$-norm. Bottom left: $L^2(H^1_{\text{av}})$-norm. Bottom right: Illustration of the numerical solution at time $t = 1$

error is zero, as the boundary $\partial \Omega^k$ consists of plane surfaces for all k. An illustration of the numerical solution at time $t = 1$ is given in the bottom right part of Fig. 5.

5.3.1 P_1 Finite Elements

As the numerical experiments in three space dimensions are much more time-consuming compared to two dimensions, we focus on simultaneous refinement in space and time by choosing $h_i = 10\Delta t_i = 2^{-i-1}$ for $i = 0, ..., 3$. The resulting errors in the three norms introduced above are plotted in Fig. 4 over the mesh size (blue curves) and compared to linear (red) and quadratic convergence (pink). We observe second-order convergence in the L^2-norms and first-order convergence in the $L^2(H^1_{av})$-norm. We note that first-order convergence in space has been shown in Theorem 4.6 in the L^2-norm at the end time and in the $L^2(H^1_{av})$-norm (under the stronger CFL condition $\Delta t \leq ch^2$). The numerical results indicate again that second-order convergence in space could be shown in the $L^2(L^2)$-norm using a duality argument. The first-order convergence in the $L^2(H^1_{av})$-norm is optimal, as the spatial error part dominates the overall error.

5.3.2 P_2 Finite Elements

In Fig. 5, we illustrate the errors under simultaneous refinement ($h_i = 10\Delta t_i$) for P_2 finite elements. We observe again (at least) second-order convergence in the L^2-norms, in agreement with Theorem 4.6. The convergence in the $L^2(H^1_{av})$-norm lies between linear and
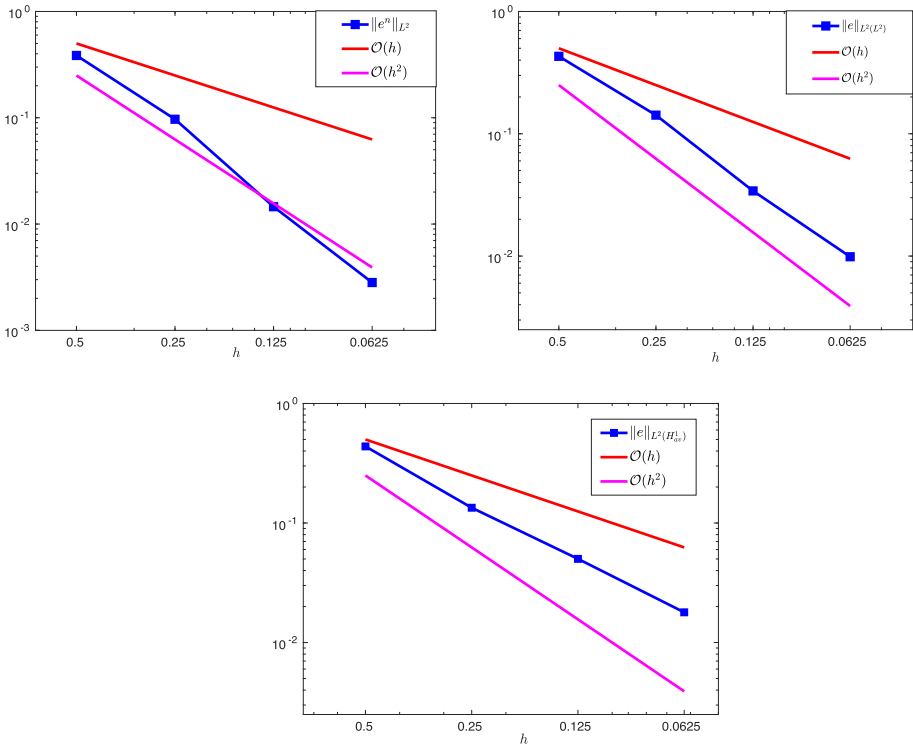
Fig. 5 Errors for example 5.2 (3d) for P_2 finite elements under simultaneous refinement in space and time ($\Delta t = h/10$) for P_1 finite elements. Top left: L^2-norm at the end time. Top right: $L^2(L^2)$-norm. Bottom: $L^2(H^1_{av})$-norm

quadratic convergence and decreases slightly for finer mesh sizes. On the finest level, we have $h_3^2 = (1/16)^2 = \frac{1}{256}$ and $\Delta t_3 = \frac{1}{10}h_3 = \frac{1}{160}$. The stronger CFL condition $\Delta t \leq ch^2$, which is needed to show optimal order of convergence, might thus be violated on this (and possibly the next coarser) level. On the other hand, we did again not observe any stability issues in our computations.

6 Concluding Remarks

We have analysed a Crank–Nicolson variant of the implicitly extended Eulerian time-stepping scheme for the heat equation on time-dependent domains. Theoretically, stability estimates were derived in the energy norm under the assumption of the CFL condition $\Delta t \leq c_{CFL}h^{3/2}$ for a sufficiently small constant c_{CFL}. Under the same condition, we obtain error estimates in the energy norm of order $\mathcal{O}(\Delta t^2 + h^{m-1/4})$, which are sub-optimal by a power of $1/4$ in space. Assuming the stronger condition $\Delta t \leq ch^2$ optimal-order error estimates in time and space have been shown. In the numerical results, on the other hand, we did not observe any stability issue related to a violated CFL condition. The three-dimensional results for second-order polynomials indicate that a violated CFL condition could result in a slightly reduced convergence order in the $L^2(H^1_{av})$-norm.

To our knowledge this is the first work, in which an implicitly extended Eulerian time-stepping scheme is applied with a scheme that requires derivative information at different time steps. As mentioned in the introduction, this could be the basis for an analysis of a whole zoo of time-stepping schemes, such as the Fractional-step-θ method, implicit Runge–Kutta- or Adams–Bashforth schemes. Moreover, we plan to apply the developed time-stepping scheme to flow problems on time-dependent domains and to fluid–structure interactions with large displacements, see e.g. [9, 27].

Data Availability The input parameters of the numerical simulations are described within the manuscript. The CutFEM library [8] used in the numerical simulations is not publicly available. Further details on the output of the numerical simulations are available from the corresponding author upon reasonable request.

Declarations

Conflict of interest The authors have no relevant financial or non-financial interests to disclose and there are no Conflict of interest that are relevant to the content of this article. All authors certify that they have no affiliations with or involvement in any organization or entity with any financial or non-financial interest in the subject matter or materials discussed in this manuscript. Moreover, we have no financial or proprietary interests in any material discussed in this article.

References

1. Alnæs, M., Blechta, J., Hake, J., Johansson, A., Kehlet, B., Logg, A., Richardson, C., Ring, J., Rognes, M.E., Wells, G.N.: The fenics project version 1.5. Arch. Numer. Soft. **3**(100) (2015). https://doi.org/10.11588/ans.2015.100.20553
2. Babuška, I., Banarjee, U., Osborn, J.E.: Generalized finite element methods: main ideas, results, and perspective. Int. J. Comput. Methods **1**, 67–103 (2004)
3. Bazilevs, Y., Takizawa, K., Tezduyar, T.E.: Computational Fluid–Structure Interaction: Methods and Applications. Wiley, Hoboken (2013)
4. Becker, R.: An adaptive finite element method for the incompressible Navier–Stokes equations on time-dependent domains. Ph.D. thesis, Habilitation Thesis, University of Heidelberg, Germany (1995)
5. Bramble, J.H., King, J.T.: A finite element method for interface problems in domains with smooth boundaries and interfaces. Adv. Comput. Math. **6**, 109–138 (1996)
6. Brenner, S.C.: The Mathematical Theory of Finite Element Methods. Springer, Berlin (2008)
7. Burman, E.: Ghost penalty. C. R. Math. **348**(21–22), 1217–1220 (2010)
8. Burman, E., Claus, S., Hansbo, P., Larson, M.G., Massing, A.: Cutfem: discretizing geometry and partial differential equations. Int. J. Numer. Methods Eng. **104**(7), 472–501 (2015)
9. Burman, E., Fernández, M.A., Frei, S.: A Nitsche-based formulation for fluid–structure interactions with contact. ESAIM: M2AN **54**(2), 531–564 (2020)
10. Burman, E., Fernández, M.A., Frei, S., Gerosa, F.M.: A mechanically consistent model for fluid–structure interactions with contact including seepage. Comput. Methods Appl. Mech. Eng. **392**, 114637 (2022)
11. Burman, E., Fernández, M.A.: An unfitted Nitsche method for incompressible fluid–structure interaction using overlapping meshes. Comput. Methods Appl. Mech. Eng. **279**, 497–514 (2014)

12. Burman, E., Frei, S., Massing, A.: Eulerian time-stepping schemes for the non-stationary Stokes equations on time-dependent domains. Numer. Math. **150**, 423–478 (2022)
13. Burman, E., Hansbo, P., Larson, M.G.: A cut finite element method with boundary value correction. Math. Comput. **87**(310), 633–657 (2018)
14. Burman, E., Hansbo, P., Larson, M.G., Zahedi, S.: Cut finite element methods for coupled bulk-surface problems. Numer. Math. **133**(2), 203–231 (2016)
15. Caucha, L.J., Frei, S., Rubio, O.: Finite element simulation of fluid dynamics and CO_2 gas exchange in the alveolar sacs of the human lung. Comput. Appl. Math. **37**(5), 6410–6432 (2018)
16. Chessa, J., Belytschko, T.: An extended finite element method for two-phase fluids. J. Appl. Mech. **70**(1), 10–17 (2003)
17. Claus, S., Kerfriden, P.: A CutFEM method for two-phase flow problems. Comput. Methods Appl. Mech. Eng. **348**, 185–206 (2019)
18. Codina, R., Houzeaux, G., Coppola-Owen, H., Baiges, J.: The fixed-mesh ALE approach for the numerical approximation of flows in moving domains. J. Comput. Phys. **228**(5), 1591–1611 (2009)
19. Crowe, C.T., Schwarzkopf, J.D., Sommerfeld, M., Tsuji, Y.: Multiphase Flows with Droplets and Particles. Taylor & Francis, Oxford (1997)
20. Daux, C., Moës, N., Dolbow, J., Sukumar, N., Belytschko, T.: Arbitrary branched and intersecting cracks with the extended finite element method. Int. J. Numer. Methods Eng. **48**(12), 1741–1760 (2000)
21. Donea, J., Giuliani, S., Halleux, J.-P.: An arbitrary Lagrangian–Eulerian finite element method for transient dynamic fluid–structure interactions. Comput. Methods Appl. Mech. Eng. **33**(1–3), 689–723 (1982)
22. Donea, J., Huerta, A., Ponthot, J.-P., Rodríguez-Ferran, A.: Arbitrary Lagrangian–Eulerian Methods. Wiley Online Library (2004)
23. Dunne, T.: An Eulerian approach to fluid–structure interaction and goal-oriented mesh adaptation. Int. J. Numer. Methods Fluids **51**(9–10), 1017–1039 (2006)
24. Feistauer, M., Sobotíková, V.: Finite element approximation of nonlinear problems with discontinuous coefficients. ESAIM: M2AN **24**, 457–500 (1990)
25. Formaggia, L., Quarteroni, A., Veneziani, A.: Cardiovascular Mathematics: Modeling and Simulation of the Circulatory System, vol. 1. Springer, Berlin (2010)
26. Frachon, T., Zahedi, S.: A cut finite element method for incompressible two-phase Navier–Stokes flows. J. Comput. Phys. **384**, 77–98 (2019)
27. Frei, S.: Eulerian finite element methods for interface problems and fluid–structure interactions. Ph.D. thesis, University of Heidelberg, Germany (2016)
28. Frei, S.: An edge-based pressure stabilization technique for finite elements on arbitrarily anisotropic meshes. Int. J. Numer. Methods Fluids **89**(10), 407–429 (2019)
29. Frei, S., Judakova, G., Richter, T.: A locally modified second-order finite element method for interface problems. ESAIM: M2AN **57**(3), 1355–1380 (2023)
30. Frei, S., Richter, T.: A locally modified parametric finite element method for interface problems. SIAM J. Numer. Anal. **52**(5), 2315–2334 (2014)
31. Frei, S., Richter, T.: A second order time-stepping scheme for parabolic interface problems with moving interfaces. ESAIM: M2AN **51**(4), 1539–1560 (2017)
32. Fries, T.-P., Belytschko, T.: The extended/generalized finite element method: an overview of the method and its applications. Int. J. Numer. Methods Eng. **84**(3), 253–304 (2010)
33. Ganesan, S., Srivastava, S.: ALE-SUPG finite element method for convection–diffusion problems in time-dependent domains: conservative form. Appl. Math. Comput. **303**, 128–145 (2017)
34. Garcke, H., Lam, K.F., Nürnberg, R., Sitka, E.: A multiphase Cahn–Hilliard–Darcy model for tumour growth with necrosis. Math. Models Methods Appl. Sci. **28**(03), 525–577 (2018)
35. Gross, S., Reusken, A.: Numerical Methods for Two-phase Incompressible Flows, vol. 40. Springer, Berlin (2011)
36. Gurris, M., Kuzmin, D., Turek, S.: Finite element simulation of compressible particle-laden gas flows. J. Comput. Appl. Math. **233**(12), 3121–3129 (2010)
37. Hansbo, A., Hansbo, P.: An unfitted finite element method, based on Nitsche's method, for elliptic interface problems. Comput. Methods Appl. Mech. Eng. **191**(47–48), 5537–5552 (2002)
38. Hansbo, P., Larson, M.G., Zahedi, S.: A cut finite element method for a Stokes interface problem. Appl. Numer. Math. **85**, 90–114 (2014)
39. Hansbo, P., Larson, M.G., Zahedi, S.: A cut finite element method for coupled bulk-surface problems on time-dependent domains. Comput. Methods Appl. Mech. Eng. **307**, 96–116 (2016)
40. Hecht, F., Pironneau, O.: An energy stable monolithic Eulerian fluid–structure finite element method. Int. J. Numer. Methods Fluids **85**(7), 430–446 (2017)
41. Hirt, C.W., Amsden, A.A., Cook, J.L.: An Arbitrary Lagrangian–Eulerian computing method for all flow speeds. J. Comput. Phys. **135**(2), 203–216 (1997)

42. Hughes, T.J., Liu, W.K., Zimmermann, T.K.: Lagrangian–Eulerian finite element formulation for incompressible viscous flows. Comput. Methods Appl. Mech. Eng. **29**(3), 329–349 (1981)

43. Hysing, S.-R., Turek, S., Kuzmin, D., Parolini, N., Burman, E., Ganesan, S., Tobiska, L.: Quantitative benchmark computations of two-dimensional bubble dynamics. Int. J. Numer. Methods Fluids **60**(11), 1259–1288 (2009)

44. Johansson, A., Larson, M.G., Logg, A.: High order cut finite element methods for the Stokes problem. Adv. Model. Simul. Eng. Sci. **2**(1), 1–23 (2015)

45. Judakova, G., Bause, M.: Numerical investigation of multiphase flow in pipelines. Int. J. Mech. Mechatron. **11**(9), 1540–1546 (2017)

46. Juntunen, M., Stenberg, R.: Nitsche's method for general boundary conditions. Math. Comput. **78**(267), 1353–1374 (2009)

47. Knauf, S., Frei, S., Richter, T., Rannacher, R.: Towards a complete numerical description of lubricant film dynamics in ball bearings. Comput. Mech. **53**(2), 239–255 (2014)

48. Lehrenfeld, C.: The Nitsche XFEM-DG space–time method and its implementation in three space dimensions. SIAM J. Sci. Comput. **37**(1), A245–A270 (2015)

49. Lehrenfeld, C., Olshanskii, M.A.: An finite element method for PDEs in time-dependent domains. ESAIM: M2AN **53**(2), 585–614 (2019)

50. Lou, Y., Lehrenfeld, C.: Isoparametric unfitted BDF-finite element method for PDEs on evolving domains. SIAM J. Numer. Anal. **60**(4), 2069–2098 (2022)

51. Massing, A., Larson, M.G., Logg, A., Rognes, M.E.: A stabilized Nitsche fictitious domain method for the Stokes problem. J. Sci. Comput. **61**(3), 604–628 (2014)

52. Massing, A., Schott, B., Wall, W.A.: A stabilized Nitsche cut finite element method for the Oseen problem. Comput. Methods Appl. Mech. Eng. **328**, 262–300 (2018)

53. Nitsche, J.A.: Über ein Variationsprinzip zur Lösung von Dirichlet-Problemen bei Verwendung von Teilräumen, die keinen Randbedingungen unterworfen sind. Abh Math Univ Hamburg **36**, 9–15 (1970)

54. Peskin, C.S.: Flow patterns around heart valves: a numerical method. J. Comput. Phys. **10**(2), 252–271 (1972)

55. Porté-Agel, F., Bastankhah, M., Shamsoddin, S.: Wind-turbine and wind-farm flows: a review. Bound. Layer Meteorol. **174**(1), 1–59 (2020)

56. Richter, T.: Fluid–Structure Interactions: Models, Analysis and Finite Elements, vol. 118. Springer, Berlin (2017)

57. Schott, B.: Stabilized cut finite element methods for complex interface coupled flow problems. Ph.D. thesis, Technische Universität München (2017)

58. Srivastava, S., Ganesan, S.: Local projection stabilization with discontinuous Galerkin method in time applied to convection dominated problems in time-dependent domains. BIT Numer. Math. **60**(2), 481–507 (2020)

59. Stein, K., Benney, R., Kalro, V., Tezduyar, T.E., Leonard, J., Accorsi, M.: Parachute fluid–structure interactions: 3-d computation. Comput. Methods Appl. Mech. Eng. **190**(3–4), 373–386 (2000)

60. Thomée, V.: Galerkin Finite Element Methods for Parabolic Problems, vol. 25. Springer, Berlin (2007)

61. Van de Vosse, F.N., De Hart, J., Van Oijen, C.H.G.A., Bessems, D., Gunther, T.W.M., Segal, A., Wolters, B.J.B.M., Stijnen, J.M.A., Baaijens, F.P.T.: Finite-element-based computational methods for cardiovascular fluid–structure interaction. J. Eng. Math. **47**(3), 335–368 (2003)

62. von Wahl, H., Richter, T., Lehrenfeld, C.: An unfitted finite element method for the time-dependent Stokes problem on moving domains. IMA J. Numer. Anal. 1–40 (2021)

63. Wall, W.A., Rabczuk, T.: Fluid–structure interaction in lower airways of CT-based lung geometries. Int. J. Numer. Methods Fluids **57**(5), 653–675 (2008)

64. Williams, T., Kelley, C., Bersch, C., Bröker, H.-B., Campbell, J., Cunningham, R., Denholm, D., Elber, G., Fearick, R., Grammes, C., et al.: gnuplot 5.2. An interactive plotting program. Available online: http://www.gnuplot.info/docs_5, 2 (2017)

65. Zahedi, S.: A space-time cut finite element method with quadrature in time. In: Geometrically Unfitted Finite Element Methods and Applications: Proceedings of the UCL Workshop 2016, pp. 281–306. Springer International Publishing (2017)